Development 138, 3943-3954 (2011) doi:10.1242/dev.067447

Biological and mathematical modeling of melanocyte development

Flavie Luciani[1,2,3], Delphine Champeval[1,2,3], Aurélie Herbette[1,2,3], Laurence Denat[1,2,3], Bouchra Aylaj[4], Silvia Martinozzi[1,2,3], Robert Ballotti[5], Rolf Kemler[6], Colin R. Goding[7], Florian De Vuyst[4,8], Lionel Larue[1,2,3,*,‡] and Véronique Delmas[1,2,3,*,‡]

SUMMARY

We aim to evaluate environmental and genetic effects on the expansion/proliferation of committed single cells during embryonic development, using melanoblasts as a paradigm to model this phenomenon. Melanoblasts are a specific type of cell that display extensive cellular proliferation during development. However, the events controlling melanoblast expansion are still poorly understood due to insufficient knowledge concerning their number and distribution in the various skin compartments. We show that melanoblast expansion is tightly controlled both spatially and temporally, with little variation between embryos. We established a mathematical model reflecting the main cellular mechanisms involved in melanoblast expansion, including proliferation and migration from the dermis to epidermis. In association with biological information, the model allows the calculation of doubling times for melanoblasts, revealing that dermal and epidermal melanoblasts have short but different doubling times. Moreover, the number of trunk founder melanoblasts at E8.5 was estimated to be 16, a population impossible to count by classical biological approaches. We also assessed the importance of the genetic background by studying gain- and loss-of-function β-catenin mutants in the melanocyte lineage. We found that any alteration of β-catenin activity, whether positive or negative, reduced both dermal and epidermal melanoblast proliferation. Finally, we determined that the pool of dermal melanoblasts remains constant in wild-type and mutant embryos during development, implying that specific control mechanisms associated with cell division ensure half of the cells at each cell division to migrate from the dermis to the epidermis. Modeling melanoblast expansion revealed novel links between cell division, cell localization within the embryo and appropriate feedback control through β-catenin.

KEY WORDS: Mitf, Dct, β-Catenin, Melanoblast, Mouse

INTRODUCTION

Mice with a defined background display a similar uniform coat color. This indicates that there is no major variation in melanocyte production during development throughout the entire body or between individuals. Therefore, the mechanisms of melanocyte production must be tightly regulated to provide a defined number of cells: initially there are a very limited number of progenitors and subsequently thousands of cells (Mintz, 1967; Wilkie et al., 2002). Melanocytes are derived from neural crest cells, a transient population of cells arising from the dorsal part of the neural tube (Le Douarin and Kalcheim, 1999). In the truncal region of the mice, founder melanoblasts are determined around E8.5-E9.5 (Pla et al., 2001; Thomas and Erickson, 2008). From E10.0, precursor melanoblasts arising from founder melanoblasts can be visualized as single cells throughout development. From E10.5, the melanoblasts begin to spread from the migration staging area (MSA) through the dermis and migrate along a dorsolateral pathway between the ectoderm and the dorsal surface of the somites (Wehrle-Haller and Weston, 1995). Initial observations by Mayer in 1973 suggested that some of these melanoblasts migrate on E13.5 from the dermis to the epidermis where they continue to proliferate and migrate actively (Mayer, 1973). Then, between E15.5 and E16.5, clusters of melanoblasts form progressively as they move into the developing hair follicles. Finally, melanocytes reside in the dorsal part of the hair matrix and their renewal after birth is assured by melanocyte stem cells in the bulge and their transit amplifying cells.

Mice with a non-uniform pigmentation pattern are the result of mutations in genes that control the melanoblast developmental program: the affected genes may be involved in determination, proliferation, migration, differentiation or other processes. Mouse mutants (natural, physically/chemically induced or genetically engineered) are an invaluable resource for identification of the key proteins that regulate melanoblast development, including proteins produced either in the developing skin or by the melanoblast itself. More than 80 genes have been specifically implicated in melanocyte development, although their precise functions and the times at which they exert their functions are in most cases unknown (Lamoreux et al., 2010) (http://www.espcr.org/micemut/#cloned). These genes encode a variety of proteins, including growth and differentiation factors, metalloproteinases, and signaling and transcription factors. These proteins are produced by melanoblasts or by cells in the surrounding environment (Yamaguchi and Hearing, 2009). Wnts are locally produced factors that are believed to play a crucial role in melanoblast determination. Inactivation of

[1]Institut Curie, Centre de Recherche, Developmental Genetics of Melanocytes, 91405 Orsay, France. [2]CNRS UMR3347, 91405 Orsay, France. [3]INSERM U1021, 91405 Orsay, France. [4]Laboratoire Mathématiques Appliquées aux systèmes, Ecole Centrale Paris, Grande Voie des Vignes, 94235 Chatenay-Malabry Cedex, France. [5]INSERM U895, Equipe 1, 28 Avenue de Valombrose, 06107 Nice Cedex 2, France. [6]Max-Planck Institute of Immunobiology, Department of Molecular Embryology, D-79108 Freiburg, Germany. [7]Ludwig Institute for Cancer Research, University of Oxford, Oxford OX3 7DQ, UK. [8]Centre de Mathématiques et de leurs applications, Ecole Normale Supérieure de Cachan, 61 Avenue du Président Wilson, 94235 Cachan Cedex, France.

*These authors contributed equally to this work.
‡Authors for correspondence (lionel.larue@curie.fr; veronique.delmas@curie.fr)

Accepted 16 June 2011

both Wnt1 and Wnt3a in mice leads to the absence of melanoblasts, whereas overexpression of Wnt1 in murine NCC results in expansion of the number of melanoblasts in vitro (Dunn et al., 2000; Ikeya et al., 1997). Specific mutation of β-catenin, the central component of canonical Wnt signaling, in NCC confirms the role of this pathway in melanoblast determination (Hari et al., 2002). However, the effect of the Wnt/β-catenin signaling pathway on melanoblast expansion and localization during development in the skin has not been investigated.

β-Catenin is central to several developmental processes. Numerous studies using genetic approaches have revealed that this protein is important in multiple cellular functions, including proliferation, cell fate, survival and differentiation (Grigoryan et al., 2008). β-Catenin is involved in a wide variety of cellular mechanisms owing to its various different binding partners and its cellular localizations at the membrane, in the cytoplasm or in the nucleus. At the plasma membrane, β-catenin is associated with cadherin and controls cell-cell adhesion. In the nucleus, β-catenin interacts with the LEF/TCF factor to regulate gene transcription and more than 100 β-catenin targets have been identified (http://www.stanford.edu/~rnusse/pathways/targets.html). In epithelial cells, gain-of-function studies using mutants with stabilized β-catenin have shown that this protein can induce cellular proliferation with frequent transformation (Grigoryan et al., 2008). In the melanocyte lineage, the expression of a stabilized form of β-catenin induces a reduction of pigmentation (Delmas et al., 2007). This hypopigmentation may be due to a reduction of melanoblast/melanocyte numbers, a reduction of melanin production and/or melanosome transport/transfer. Some β-catenin targets, such as c-myc and cyclin D1, induce proliferation and are ubiquitously produced. Moreover, in melanocytes and in melanoma in culture, β-catenin directly regulates the expression of *Mitf-M* (the M form of the microphthalmia protein) (Dorsky et al., 2000; Takeda et al., 2000). Mitf-M is a basic helix-loop-helix zipper transcription factor restricted to neural crest-derived melanocytes and considered to be the master gene of this lineage. Depending on *MITF-M* gene activity, the protein affects proliferation by inducing *Met*, *Cdk2*, *p21* and *p16*: Met and Cdk2 induce proliferation and p21, and p16 induces cell cycle-arrest (Carreira et al., 2005; Du et al., 2004; Loercher et al., 2005; McGill et al., 2006). Moreover, Mitf-M may interact with LEF1 or with β-catenin, affecting their transcriptional activities (Schepsky et al., 2006; Yasumoto et al., 2002).

The aim of this study was to evaluate the spatial and temporal distribution of melanoblasts in dermis and epidermis during mouse development and to examine the cell-autonomous aspect of melanoblast proliferation in wild-type and β-catenin mutant animals.

MATERIALS AND METHODS

Transgenic mice

Mice with a conditional deletion of the gene encoding β-catenin (*Ctnnb1*) were generated by mating Tyr::Cre transgenic mice (Delmas et al., 2003) with animals homozygous for a floxed allele of β-catenin, with LoxP sites flanking exons 2 to 6 (Δbcat) (Brault et al., 2001). The construction of transgenic mice producing stabilized β-catenin in melanocytes has been described previously (Delmas et al., 2007). All mutant and transgenic mice were backcrossed more than ten times to C57BL/6. All animals were housed in specific pathogen-free conditions at Institut Curie, in line with French and European Union law.

Whole mount and skin sections

The bcat* and Δbcat mice were crossed with Dct::lacZ (Mackenzie et al., 1997) and Rosa26R mice (Soriano, 1999), and the resulting embryos were collected. The number of *lacZ*-positive cells (melanoblasts) was determined on each side of embryos (Yajima et al., 2006). Skin from 1-week-old mice was fixed in 4% paraformaldehyde, dehydrated and embedded in paraffin. Paraffin-embedded sections (7 μm) of skin or of a carefully orientated embryo were stained with Hematoxylin and Eosin, and examined by light microscopy.

Quantification of melanin

Melanin content in hair follicles was measured by spectrophotometry. Hairs were collected and weighed, and 1.5 mg samples were treated with 1.5 ml of 1 M sodium hydroxide at 85°C for 4 hours to dissolve the melanin; absorbance was measured at 475 nm (Larue et al., 1993).

Immunostaining

Melanocyte proliferation was analyzed by BrdU labeling in vivo, with embryos at various stages of development. The mother was given two 50 μg/ml BrdU injections at 20-minute intervals and killed 2 hours later. Embryos were collected and fixed by overnight incubation in 4% PFA. They were incubated in 30% sucrose for 12 hours, and then 30% sucrose with 50% OCT compound for 5 hours and finally in 100% OCT. For immunofluorescence, sections were treated as described elsewhere (Puig et al., 2009). Conventional fluorescence photomicrographs were obtained with a Leica DM IRB inverted routine microscope or a Leica confocal laser scanning microscope. Figures were assembled with ImageJ. The Mann-Whitney test was used to compare groups and the significance of differences is indicated: ****$P<10^{-5}$; ***$P<10^{-4}$; **$P<10^{-3}$; *$P<10^{-2}$; ns, non significant.

Cell culture, transfection and adenovirus infection

HEK293 cells and FO-1 cells were cultured in Dulbecco's minimal essential medium supplemented with 10% of fetal calf serum. Cells were transiently transfected as previously described (Delmas et al., 2007). Adenoviruses containing gfp alone or gfp and Mitf have been described elsewhere (Gaggioli et al., 2003).

Mathematical model construction and methodology

Two balance equations involving the cell flux from the dermis to epidermis, which is unknown, are given:

$$\frac{dn_{d,\theta}}{dt} = \mu_{d,\theta}(t)n_{d,\theta}(t) - \Phi_\theta\left(t, n_{d,\theta}(t), n_{e,\theta}(t)\right) \quad (1)$$

$$\frac{dn_{e,\theta}}{dt} = \mu_{e,\theta}(t)n_{e,\theta}(t) + \Phi_\theta\left(t, n_{d,\theta}(t), n_{e,\theta}(t)\right). \quad (2)$$

According to our observations (see Appendix in the supplementary material), we have two important pieces of information: (1) the total number of melanoblasts, n_θ, increases exponentially; and (2) the progress of fraction of melanoblasts in the dermis, y_θ, through time is sigmoidal (or S-shaped). Consequently, we can establish equations for n_θ and y_θ, both unknown variables of interest, which are now linked to two equations. The y_θ equation involves the rate of decrease of the fraction of melanoblasts in the dermis:

$$\frac{dy_\theta}{dt} = -c_\theta(t)y_\theta(t)\left(1 - y_\theta(t)\right) \quad (13)$$

and y_θ itself. The n_θ equation involves the rate of increase of melanoblasts in the dermis and epidermis:

$$\frac{dn_\theta(t)}{dt} = \mu_\theta(t)n_\theta(t) \quad (14)$$

and n_θ itself. The two rates involved in the y_θ and n_θ equations can be estimated from the experimental data:

$$c_\theta(t) = d\log(n_{e,\theta}(t) / n_{d,\theta}(t)) / dt \quad (7)$$

and

$$d\log(n_\theta(t)) / dt = \mu_\theta(t)\,. \quad (6)$$

After 'feeding' the Eqns 13 and 14 with the experimental data, these two novel equations are independent of the melanoblast flux. The explanation of the 'feeding' is given elsewhere (Aylaj et al., 2011). Note that y_θ and n_θ

fit the experimental data almost perfectly. Now, we have three unknowns (growth rate in the dermis, growth rate in the epidermis and the flux factor) and two equations:

$$\hat{c}_\theta(t) = \kappa_\theta(t) + \mu_{e,\theta}(t) - \mu_{d,\theta}(t) \quad (4)$$

and

$$\hat{\mu}_\theta(t) = (y_\theta(t))\mu_{d,\theta}(t) + (1 - y_\theta(t))\mu_{e,\theta}(t) . \quad (5)$$

The 'third equation' for the three unknowns can be generated from the confidence interval for the flux factor:

$$\kappa_\theta \min(t) \leq \kappa_\theta(t) \leq \kappa_\theta \max(t) \quad (10)$$

(see Appendix in the supplementary material). In conclusion, the problem can by solved through a probabilistic approach.

RESULTS

Spatial and temporal melanoblast distribution during development

To study in detail the patterns of melanoblast expansion during development, we used the Dct::lacZ reporter mice in the C57BL/6 background; in these mice, melanoblasts can be labeled with X-gal from E10.5 onwards (Fig. 1A). We determined the number of melanoblasts in the truncal region covering somites 13-25 (Fig. 1B). A box and whiskers plot was used to indicate the degree of dispersion and the skewness of the data (Fig. 1C). Melanoblasts were evenly distributed in the truncal region of all embryos analyzed, and the map of the progression of melanoblasts did not vary substantially between embryos at any stage of development. The numbers of melanoblasts differed by a factor of less than two between embryos, with a mean and a median that were almost identical. The logarithm in base 2 (Ln2) of the number of melanoblasts was plotted against developmental stage and non-linear regression used (Fig. 1D). The mean number of melanoblasts followed a perfect exponential expansion with a correlation coefficient (r) of 0.99931, which places the correlation into the 'strong' category. The overall melanoblast doubling time (τ) was determined from the exponential regression equation where the exponent, 1.0275, represents $(\mathrm{Ln2}/\tau)^{-1}$: the doubling time between E10.5 and E15.5 was 0.67 days (16 hours).

Whole-mount studies give a general view of melanoblast development but do not allow the visualization of melanoblasts specifically in the two skin compartments: the epidermis and dermis. Therefore, we prepared transverse sections from the truncal region and X-gal-stained melanoblasts (Fig. 2A). For each stage, melanoblasts were counted in each section and recorded according to their location (Fig. 2B,C). In the epidermis, the number of melanoblasts per section increased with time (from 0 to 320), whereas in the dermis, the number of melanoblasts per section

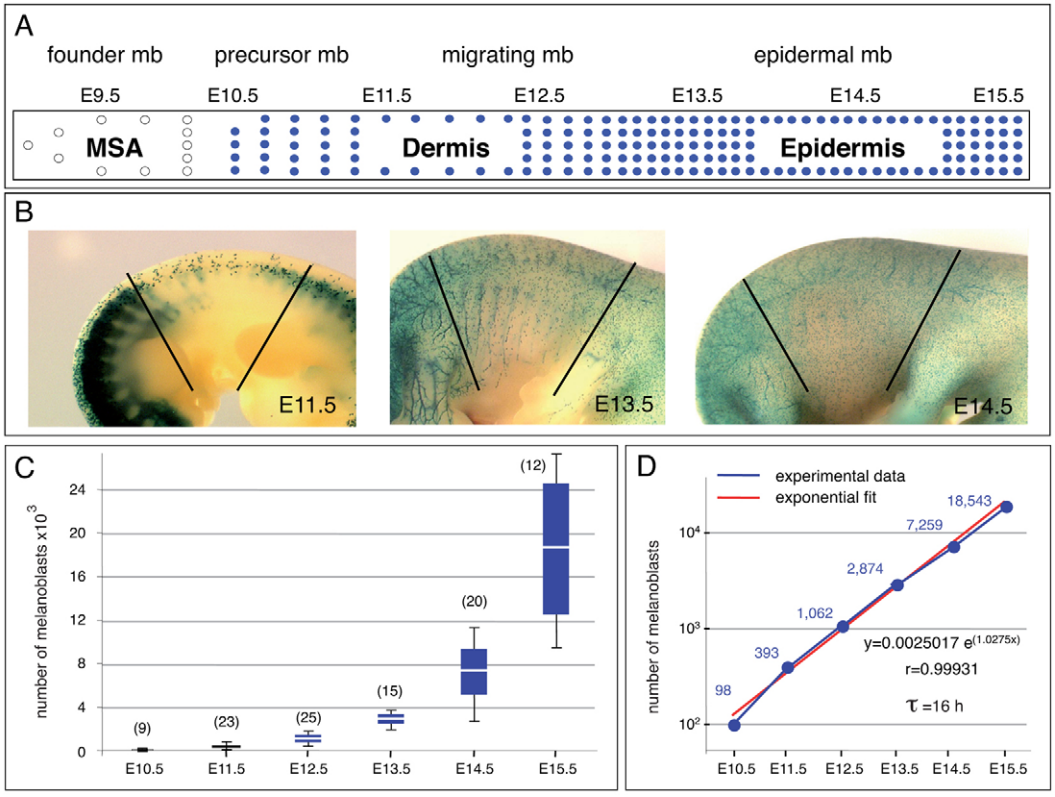

Fig. 1. Quantification of melanoblast numbers and doubling time of melanoblasts during development. (**A**) Spatiotemporal view of mouse embryo truncal melanoblasts from embryonic day 9.5 (E9.5) to E15.5. Blue and white dots correspond to melanoblasts (mb) expressing or not expressing *lacZ* under control of the Dct promoter, respectively. (**B**) Macroscopic observations of *Dct::lacZ* embryos at E11.5, E13.5 and E14.5, with the melanoblasts stained with X-gal for β-galactosidase activity. Note that the melanoblast density in the invaded region does not increase significantly from E13.5 to E15.5. (**C**) Box and whiskers plot of melanoblast numbers during development. Values are numbers of melanoblasts on two sides of the embryo in the trunk region between the front and back limbs (somites 13-25, limits shown as black lines in photographs in B). The number of embryos counted is indicated in brackets, and means are represented by white lines in the blue boxes. Bars indicate the non-atypical minimum and maximum for each day of development. (**D**) The log number of melanoblasts plotted against the time of development. The plot is perfectly linear, and allows the determination of melanoblast doubling time (τ), which is given in hours. MSA, migrating staging area.

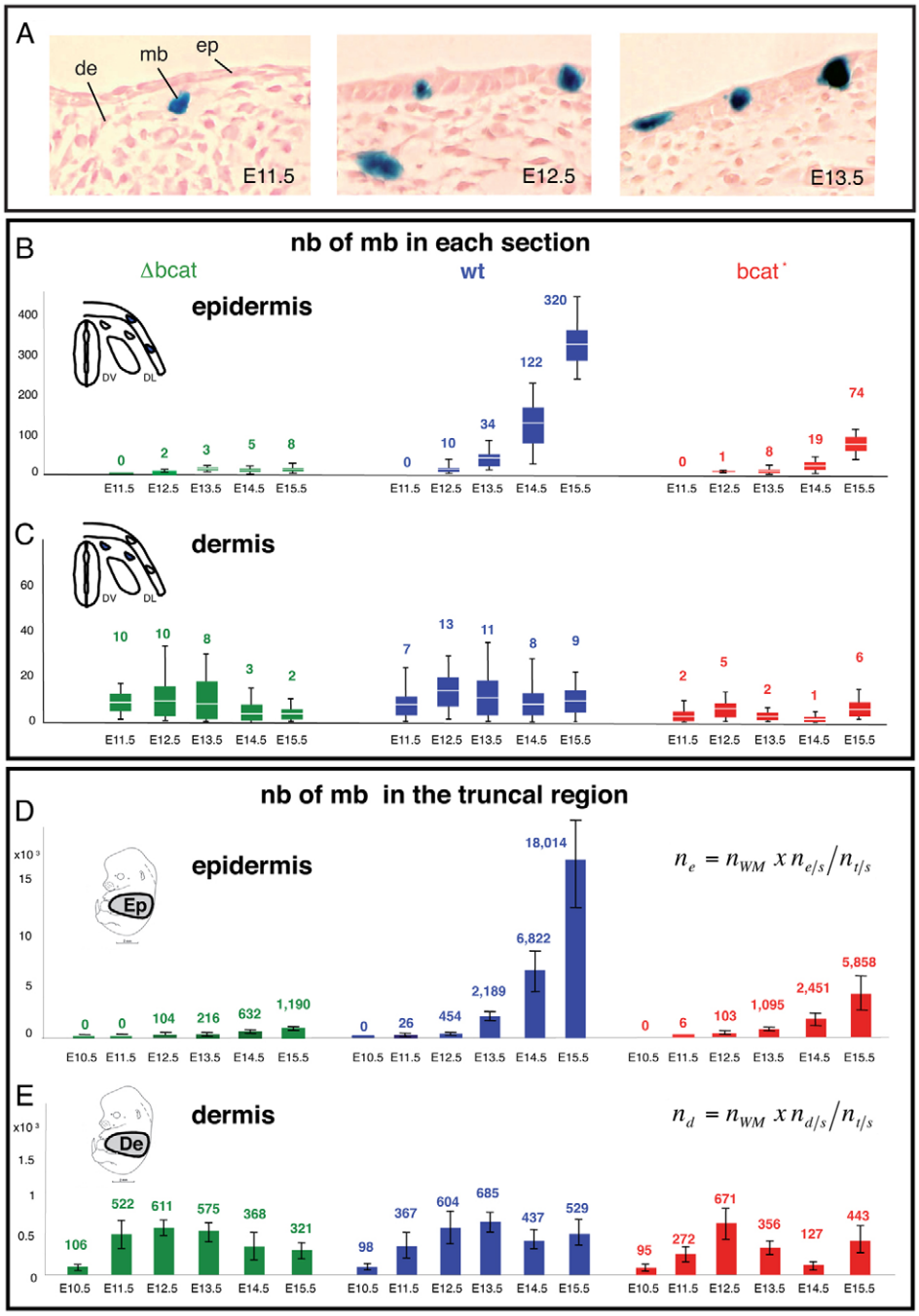

Fig. 2. Dermal and epidermal distribution of melanoblasts. (**A**) Sections through the trunk of embryos at E11.5, E12.5 and E13.5. Melanoblasts (mb), identified as X-gal-positive cells, are observed in both compartments of the skin: epidermis (ep) and dermis (de). (**B**,**C**) The number of epidermal (B) and dermal (C) melanoblasts per section was determined between embryonic days E11.5 and E15.5 between the two limbs for β-catenin loss-of-function (Δbcat in green), wild-type (wild type in blue) and gain-of-function (bcat* in red) embryos. The mean cell number is represented by the white line in colored boxes and is indicated above. Bars indicate the non-atypical minimum and maximum for each day of development. (**D**,**E**) The total number of epidermal (D) and dermal (E) melanoblasts was estimated from E10.5 onwards (see details in Fig. S1 and Table S1 in the supplementary material). n_e and n_d are the number of melanoblasts in epidermis and dermis, respectively, on a given embryonic day. n_{WM} denotes the mean number of melanoblasts defined by whole mount. $n_{e/s}$, $n_{d/s}$ and $n_{t/s}$ are the mean number of epidermal (*e*), dermal (*d*) and total (*t*=*e*+*d*) melanoblasts per section (*s*), respectively. Error bars indicate s.d.

remained fairly constant over time (from 7 to 13). We used these data to estimate the total melanoblast population in the epidermis and dermis in the truncal region at each stage of development: we multiplied the total number of melanoblasts (defined by the whole mount study, see Fig. 1) by the percentage of melanoblasts present in the relevant compartment and divided by 100 (see Fig. S1 and Table S1 in the supplementary material; Fig. 2D,E). For example, E12.5 embryos contained a mean of 1062 melanoblasts in the truncal region and 42.7% of them were located in the epidermis. Therefore, the epidermis contained (1062×42.7/100) 454 melanoblasts in this defined area. The results indicated substantial melanoblast expansion in the epidermis throughout development and in the dermis during two distinct phases. From E10.5 to E12.5, a phase of expansion of melanoblasts was observed, followed by a plateau (Fig. 2D,E). By E13.0, more than half the melanoblasts were located in the epidermis (see Table S1 and Fig. S2 in the supplementary material). We next analyzed whether this pattern of melanoblast development was influenced by altering the level of β-catenin, a protein that controls numerous cellular process in various cell lineages during development.

β-Catenin levels affect pigmentation

We investigated the function of β-catenin in the melanocyte lineage in vivo, using a genetic approach involving somatic loss- and gain-of-function of the gene once melanoblasts are determined. Mice lacking β-catenin (*Tyr::Cre/°; β-catenin*$^{lox(ex2\text{-}6)/lox(ex2\text{-}6)}$=Δbcat)

and mice producing a low level of stabilized β-catenin (*Tyr::*β-*cat*/°*=bcat*) in melanocytes were generated in a C57BL/6 background. We first determined the effect of the protein on coat color. Both β-catenin mutants had an altered coat color: Δbcat mice had a white coat and bcat* mutants had a gray coat (Fig. 3A). Sections from 1-week-old pups revealed gray pigmentation in the hair bulb of bcat* mice, rather than the dark pigmentation of the wild type. Pigmentation was absent from Δbcat mice (Fig. 3B). Hairs from transgenic bcat* mice had lighter pigmentation than wild type (Fig. 3C), although the melanin was distributed uniformly from the root to the apex as observed for wild-type hairs. This indicates that the transfer of melanin from the melanocytes to the keratinocytes was not altered. The hypopigmentation resulted from smaller amounts of melanin in transgenic bcat* than wild-type hairs (Fig. 3D). Melanin was absent from Δbcat hairs. Therefore, it is likely that the hypopigmentation of the coat observed in the β-catenin mutants was due to abnormally low pigment production, rather than to defects either in the distribution of melanin or in melanin transfer to the keratinocyte and hair shaft. Tail and ear pigmentation of β-catenin mutant mice was similar to that of the coat: gray for bcat* and white for Δbcat (Fig. 3E and data not shown).

Melanoblast expansion in the epidermis is strongly altered in both β-catenin mutants

We tested whether the pigmentation deficiency in β-catenin mutant mice was associated with an abnormally small number of melanocytes. We determined the number of melanoblasts produced during development of the melanocyte lineage in mice generated by crossing Dct::lacZ/° mice (=Dct::lacZ mice) with bcat* and Δbcat mice (Fig. 4). On E10.5, when the transgenes (bcat* and Cre) start their expression, the numbers of melanoblasts were similar in all mice. By E11.5, there were fewer melanoblasts in bcat* than in wild-type embryos; this difference increased with time. From E12.5, the number of melanoblasts in Δbcat mice was lower than in wild type. Overall, the number of Δbcat, wild-type and bcat* melanoblasts increased at each stage but the rates of increase differed between the genotypes. The differences in numbers of melanoblasts present during development reflected the differences in coat color observed between the genotypes after birth. Consequently, the number of melanoblasts seemed to account for the coat-color phenotype.

We analyzed the number of melanoblasts in epidermis and dermis for each genotype to determine the potential differences in expansion in the two compartments. We calculated the total number of melanoblasts in epidermis and dermis as described above (see Fig. S1 and Table S1 in the supplementary material). In the epidermis, the number of melanoblasts increased with time. The most substantial increase was in wt mice and the smallest in Δbcat mice (Fig. 2B,D). In the dermis, the total numbers of melanoblasts remained low for all genotypes, but was nevertheless smallest in β-catenin mutants (Fig. 2C,E). Overall, melanoblast numbers in the epidermis and dermis of β-catenin mutants were lower than in the wild type. However, the effect of β-catenin mutants was greater in the epidermis than in the dermis. This suggests that melanoblast expansion is particularly dependent on β-catenin signaling in the epidermal compartment.

β-Catenin level affects the proliferation of melanoblasts

The reduction of melanoblast number in β-catenin mouse mutants could be a consequence of several cellular processes: increased apoptosis, loss of differentiation, transdifferentiation (changes in cell fate) and/or decreased proliferation. The number of apoptotic melanoblasts was determined by testing for the presence of cleaved caspase 3 in β-catenin mutants and wild-type embryos from E12.5 to E14.5 (see Fig. S3 in the supplementary material). No apoptotic melanoblasts were detected in the epidermis in wild-type or in β-catenin mutants. Very few apoptotic melanoblasts were found in the dermis of wild type and β-catenin mutants at E12.5 and E13.5. It appears that the amount of apoptosis did not significantly differ between in Δbcat, wild-type and bcat* melanoblasts. Similar results were obtained by TUNEL (data not shown). We previously showed

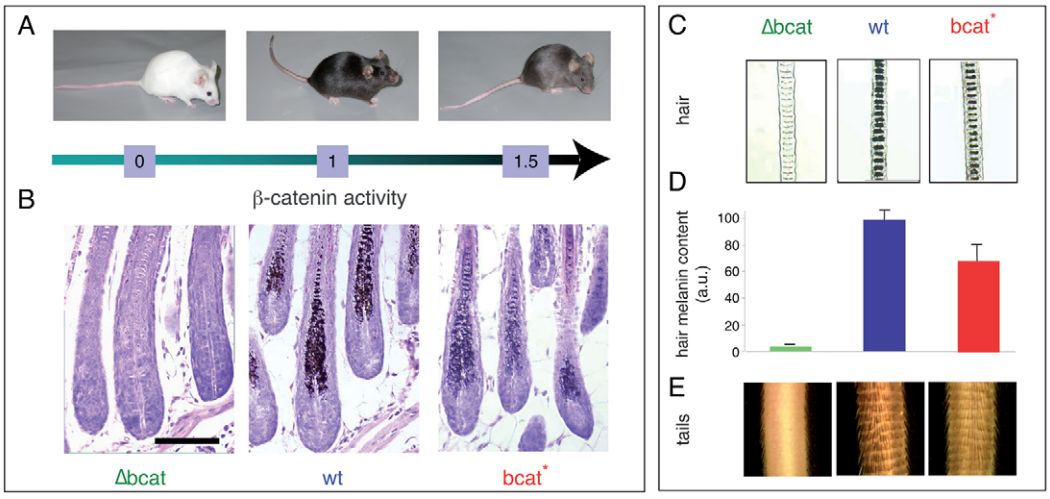

Fig. 3. β-Catenin activity controls hair pigmentation. (**A**) Photograph of β-catenin loss-of-function (white), wild-type (black) and gain-of-function (gray) adult mice. (**B**) Histological section of 1-week-old skin with Hematoxylin and Eosin staining. Note the pigmentation of hair follicles: white (Δbcat), black (wt) and gray (bcat*). (**C**) Macroscopic observations of dorsal hair follicles for the three genotypes. The pigmentation matches the corresponding hair follicles exactly. Note that pigmentation is regular and homogeneous for each hair. (**D**) Spectrophotometric measurement indicates a lower than wild-type melanin content in bcat* hair and an absence of melanin from Δbcat hair. Data are mean±s.e.m. (**E**) Tail photographs for the three genotypes.

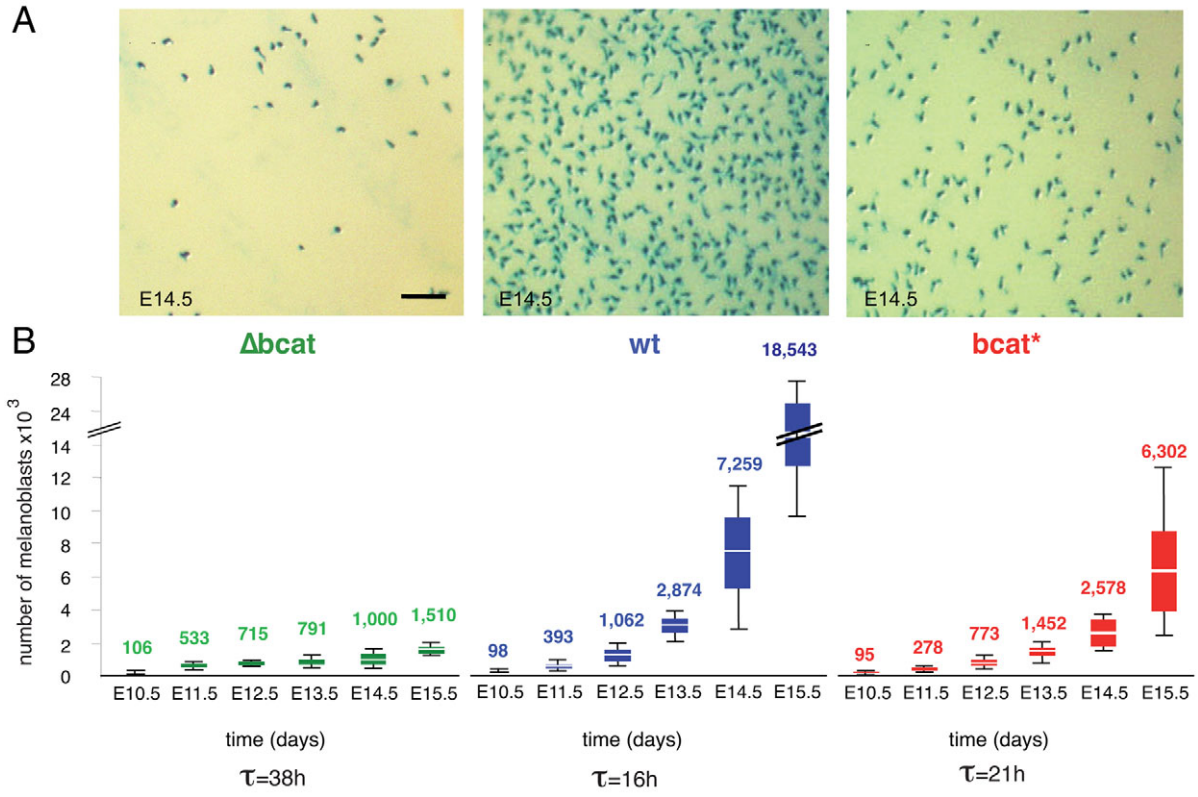

Fig. 4. β-Catenin activity affects melanoblast production. (**A**) Macroscopic observations of the trunk region of Δbcat, wild-type and bcat* E14.5 embryos. Note that melanoblasts are less abundant in both β-catenin mutants than in wild type, and in Δbcat than in bcat*. Scale bar: 100 μm. (**B**) The number of X-gal-positive cells in Δbcat, wild type and bcat* from E10.5 to E15.5 was determined by eye on both sides of embryos in the trunk region. The mean X-gal-positive cell number is shown by the white line in the colored boxes and is given above them; the non-atypical minimum and maximum are shown for each day of development by the vertical bars. Melanoblast doubling times (τ) were determined (as in Fig. 1) and indicated for each type of mutant and wild-type mice.

that no transdifferentiation or loss of commitment was observed for bcat* melanoblasts (Delmas et al., 2007). We then analyzed differences in the fate of melanoblast-committed cells between those lacking β-catenin (Δbcat) and wild type. We compared the numbers of blue cells in *Dct::lacZ* (staining for melanoblasts) and *Tyr::Cre/°; Rosa26R/+* (staining for defloxed cells) embryos. There was no difference between the two genetic backgrounds, suggesting that the absence of β-catenin did not affect cell differentiation or fate (data not shown). To test whether the coat color phenotype of Δbcat and bcat* mutants is a consequence of a reduction of melanoblast proliferation, we carried out bromodeoxyuridine (BrdU) labeling assays on embryos collected from E12.5 to E14.5. The numbers of BrdU-labeled melanoblasts were determined in epidermis and dermis for each genotype (Fig. 5). In the epidermis, for each developmental stage analyzed, the number of BrdU-positive melanoblasts was lower in β-catenin mutants than in wild type. The difference was greater for the cells lacking β-catenin than for those that expressed the stabilized form of β-catenin. In the wild-type embryos, a lower percentage of dermal melanoblasts than of epidermal melanoblasts had incorporated BrdU. This suggests that the proliferation rate is higher in the epidermis than in the dermis. A similar difference was also observed for bcat* melanoblasts, but it was less pronounced than for wild type. Finally, Δbcat melanoblasts presented an overall low level of BrdU incorporation in both compartments. These findings reveal that the proliferation of wild-type melanoblasts is faster than that of bcat* melanoblasts, and much faster than that of Δbcat melanoblasts. In conclusion, the lower numbers of Δbcat and bcat* melanoblasts are mainly due to a reduction of proliferation, and not due to apoptosis, loss-of-differentiation or transdifferentiation.

Modeling melanoblast proliferation in the skin during development

To investigate Δbcat, wild-type and bcat* melanoblast proliferation in developing skin, we developed a mathematical model to estimate the doubling time of dermal and epidermal melanoblasts. In the truncal region, founder melanoblasts are determined from the neural crest around E8.5-E9.5 and can be easily detected from E10.5 in a Dct::lacZ background. In both compartments, dermal and epidermal melanoblasts can theoretically undergo proliferation, apoptosis, loss-of-differentiation or/and transdifferentiation. Moreover, melanoblasts cross the basement membrane from the dermis to the epidermis but there is no evidence of a reverse flow of melanoblasts from epidermis to dermis in normal conditions. We showed that melanoblasts do not die, do not transdifferentiate and do not lose their differentiation. On the basis of these findings, we constructed a simplified model of melanoblast proliferation as depicted in Fig. 6A,B and detailed in the Appendix in the

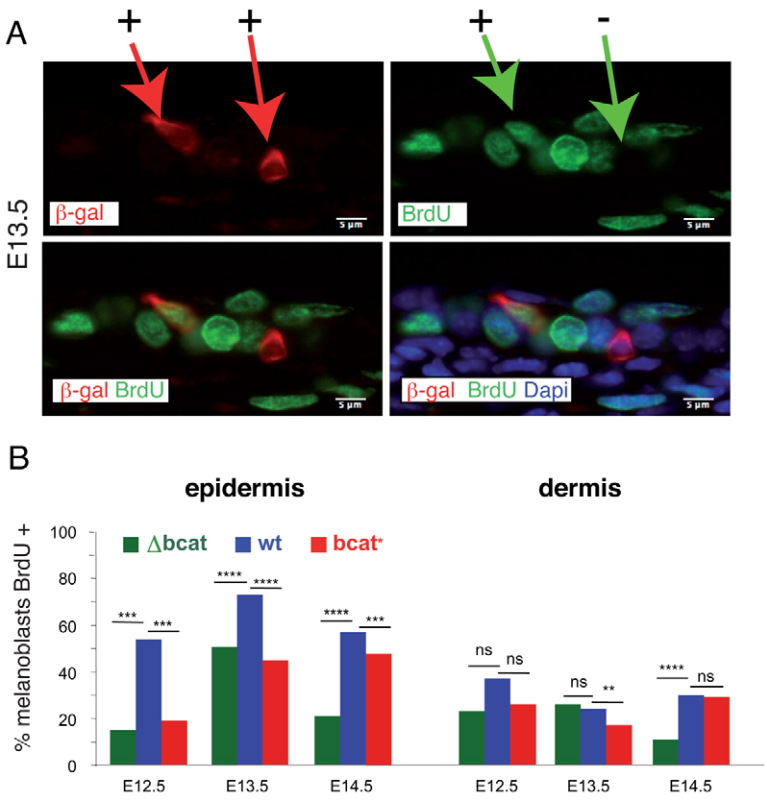

Fig. 5. Melanoblast proliferation is dependent on β-catenin signaling. (**A**) Immunostaining of *Dct::lacZ* embryo using anti-β-galactosidase (red), anti-BrdU (green) antibodies and DAPI (blue). Images are merged to reveal proliferating melanoblasts. (**B**) Determination of proliferation rate for *Dct::lacZ*-positive cells between E12.5 and E14.5 in Δbcat, wild-type and bcat* embryos. Between 20 and 107 sections, derived from two to four embryos from independent litters, were analyzed for each embryonic stage and each genotype. Statistical significance was calculated with the Mann-Whitney test and is indicated: ****$P<10^{-5}$, ***$P<10^{-4}$, **$P<10^{-3}$, ns, non significant.

supplementary material (Eqns 1-19). The number of founder melanoblasts, which are located in the MSA is $n_{d,\theta}$ (0), which is equal to n^0. At that time, there are no melanoblasts in the developing epidermis, i.e. $n_{d,\theta}$ (0)=0. The numbers of melanoblasts (n) in the dermis (d) and epidermis (e) at a particular time (t) of development are $n_{d,\theta}$ (t) and $n_{e,\theta}$ (t), respectively, with n_θ (t) = $n_{d,\theta}$ (t) + $n_{e,\theta}$ (t). The parameter θ represents the dependence on β-catenin activity. The flow Φ(t) of melanoblasts from the dermis to epidermis is, unfortunately, unknown and cannot currently be determined experimentally. We have three initial unknowns, which are the two doubling times (τ_θ) of the melanoblasts (that in the dermis and that in the epidermis) and the flow of the cells from the dermis to the epidermis. We have determined two values: the numbers of melanoblasts in the dermis and epidermis at a given time. These two values are not sufficient to solve the problem. The flow of melanoblasts from the dermis to the epidermis cannot be determined experimentally for technological reasons. Therefore, we estimated several cellular characteristics (whether the cells are or are not cycling, relative rates of proliferation, apoptosis and transdifferentiation/loss-of-differentiation), and used these data to solve the problem. Rather than three required equations to determine the three unknowns, two equations (Eqns 1 and 2), which can be obtained easily, were used. Thus, the rationale of the mathematical model was to link the doubling times τ_θ (t) [or proliferation rate μ_θ (t), $\tau_{d,\theta}$ (t) = log(2)/$\mu_{d,\theta}$ (t), $\tau_{e,\theta}$ (t) – log(2)/$\mu_{e,\theta}$ (t) Eqn 3] with the flow of the cells [or the flow factor κ_θ (t)] on the basis of the relationship of compatibility existing between unknowns κ_θ (t) = c_θ (t) – $\mu_{e,\theta}$ (t) + $\mu_{d,\theta}$ (t) (Eqn 4) (see Appendix in the supplementary material) (Aylaj et al., 2011). These unknowns can be defined as follows: $\mu_{e,\theta}$ (t) is the rate of proliferation of melanoblasts in the epidermis, corresponding to the inverse of the doubling time in the epidermis $\mu_{e,\theta}$ (t) = log(2)/$\tau_{e,\theta}$ (t) (Eqn 3), $\mu_{d,\theta}$ (t) is the rate of proliferation of melanoblasts in the dermis, corresponding to the inverse of the doubling time in the dermis $\mu_{d,\theta}$ (t) = log(2)/$\tau_{d,\theta}$ (t) (Eqn 3), κ_θ (t) represents the speed at which a melanoblast crosses from the dermis to epidermis, and c_θ (t) represents the rate of decline in the number of dermal melanoblasts. The global rate of melanoblast proliferation μ_θ (t) can be broken down into the rate of proliferation of the dermal melanoblast fraction y_θ (t) and the rate of proliferation of the epidermal melanoblast fraction (1 – y_θ (t)): μ_θ (t) = (y_θ (t))$\mu_{d,\theta}$ (t)+(1 – y_θ (t)) $\mu_{e,\theta}$ (t) (Eqn 5). The values of y_θ (t) are given in Table S1 in the supplementary material. μ_θ (t) can be calculated from the total number of melanoblasts n_θ defined biologically using the differential equation μ_θ (t)=$d$log (n_θ(t))/dt (Eqn 6), c_θ (t) can be calculated from the number of melanoblasts in the epidermis (n_e) and in the dermis (n_d) defined biologically using the differential equation c_θ (t) = $d$log($n_{e,\theta}$ (t)/$n_{d,\theta}$ (t))/dt (Eqn 7). These two differential equations were solved using MATLAB. Note that the mathematical model fits the biological data (Fig. 6B). If we were able to measure κ_θ (t), we would be able to determine $\mu_{e,\theta}$ (t) and $\mu_{d,\theta}$ (t) from the equations $\mu_{e,\theta}$ (t) = μ_θ (t) + y_θ (t) (c_θ (t) – κ_θ (t)) (Eqn 8), and $\mu_{d,\theta}$ (t) = μ_θ (t) – (1– y_θ (t)) (c_θ (t) – κ_θ (t)) (Eqn 9), which are derived from Eqns 4 and 5. Therefore, we now have two equations with three unknowns. As stated above, we cannot determine κ_θ (t) from biological experiments. However, it is possible to estimate lower and upper bounds for κ_θ (t) (κ_θ min (t) and κ_θ max (t) from biological information, and in particular the BrdU incorporation experiment which indicates the proliferation rate of melanoblasts (Fig. 5; see Fig. S4 in the supplementary material). We established two limits for $\mu_{e,\theta}$ (t) and $\mu_{d,\theta}$ (t): the proliferation rate in the epidermis is (1) greater than or equal to that in the dermis $\mu_{e,\theta}$ (t) ≥ $\mu_{d,\theta}$ (t) and (2) equal to or less than three times that in the dermis 3 $\mu_{d,\theta}$ (t) ≥ $\mu_{e,\theta}$ (t). These biological limits

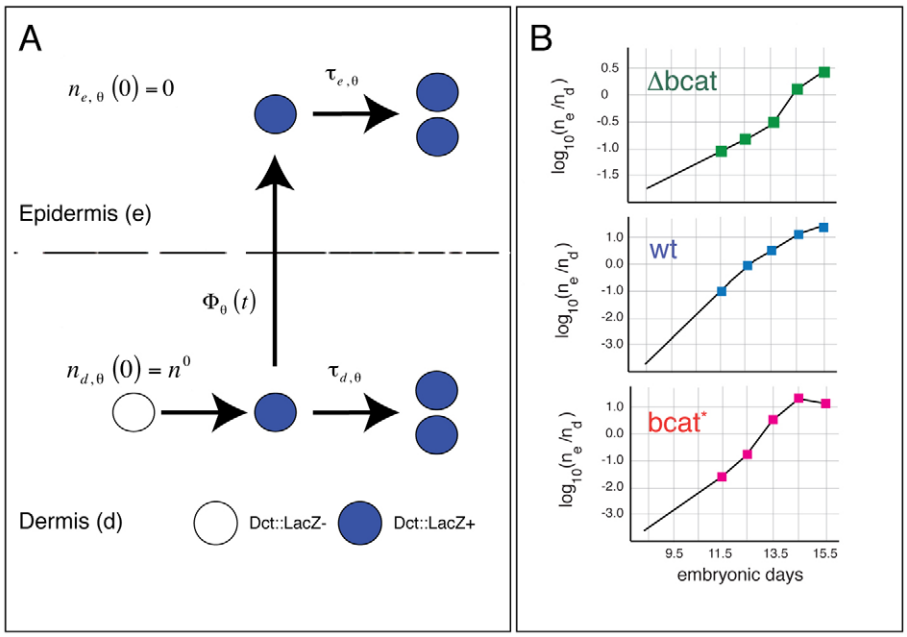

Fig. 6. Estimation of epidermal and dermal melanoblast doubling times for each genotype from a mathematical model. (**A**) Melanoblast fate in epidermis and dermis. In the dermis, *Dct::lacZ*$^+$ cells (blue) arise from *Dct::lacZ*$^-$ cells (white). The number of melanoblasts at the initial time point (E8.5), is represented by $n_{d,\theta}(0) = n^0$ for the dermis and $n_{e,\theta}(0) = 0$ for the epidermis. The parameter θ represents the dependence on β-catenin activity. The flow, $\Phi_\theta(t)$ of melanoblasts from the dermis to epidermis is, unfortunately, unknown. (**B**) Comparison between data and solution of the ratio model $\log_{10}(n_{e,\theta}(t)/n_{d,\theta}(t))$. Comparison between measurements (squares) and mathematical model (solid line) after parameter identification. Ratio of epidermal to dermal melanoblasts for Δbcat (green), wild-type (blue) and bcat* (red) mice.

are not stringent and allow high flexibility of the model. We introduced these biological limits ($\mu_{e,\theta}(t) \geq \mu_{d,\theta}(t)$, $3\,\mu_{d,\theta}(t) \geq \mu_{e,\theta}(t) \geq \mu_\theta(t)$) into Eqns 4 and 9, and thereby generated Eqn 10: $\kappa_\theta \min(t) \leq \kappa_\theta \leq \kappa_\theta \max(t)$, where $\kappa_\theta \min(t) = \max(0, c_\theta(t) - 2\mu_\theta(t)/3 - 3\,y_\theta(t))$ (Eqn 11) and $\kappa_\theta \max(t) = c_\theta(t)$ (Eqn 12) (see Fig. S4 in the supplementary material). As the value of $c_\theta(t)$ is known, $\kappa_\theta \max(t)$ can be determined. Similarly, as $\mu_\theta(t)$ and $y_\theta(t)$ are known, $\kappa_\theta \min(t)$ can be determined. The minimum and maximum rates of proliferation of melanoblasts in the epidermis ($\mu_{e,\theta} \min(t)$, $\mu_{e,\theta} \max(t)$) and dermis ($\mu_{d,\theta} \min(t)$, $\mu_{d,\theta} \max(t)$) can be determined from the known $\kappa_\theta \min(t)$ and $\kappa_\theta \max(t)$ from the following equations:

$$\mu_{e,\theta} \max(t) = \mu_\theta(t) + y_\theta(t)\,(c_\theta(t) - \kappa_\theta \min(t))\,,$$

$$\mu_{e,\theta} \min(t) = \mu_{d,\theta} \max(t) = \mu_\theta(t) \text{ and}$$

$$\mu_{d,\theta} \min(t) = \mu_\theta(t) - (1 - y_\theta(t))\,(c_\theta(t) - \kappa_\theta \min(t))\,.$$

To the extreme, the minimum doubling times in the epidermis are equal to the doubling times in the dermis, although this depends on the non stringent limits that we decided. The average rate of proliferation is simply calculated from the minimum and maximum rates of proliferation with $\mu_\theta \text{ mean}(t) = (\mu_\theta \min(t) + \mu_\theta \max(t))/2$. The average doubling time is the inverse of the average rate of proliferation (Eqn 3) and is presented in Table 1. At E14.5, the doubling time for wild-type epidermal melanoblasts was estimated by this model to be 18 hours. By analyzing whole mounts, we estimated that the doubling time of the melanoblasts to be 16 hours (Fig. 1). The results obtained from whole-mount data and from the mathematical model are thus in agreement. Moreover, from E13.5, most of the melanoblasts are located in the epidermis, and therefore the doubling time estimated from the whole mount principally reflects the proliferation of epidermal melanoblasts. At E14.5, the doubling time for wild-type dermal melanoblasts was estimated to be 28 hours (Table 1). Mathematical (28 hours versus 18 hours) and biological (BrdU experiments) data show that the doubling time in the dermis is longer than that in the epidermis. Indeed, the biological data indicate that melanoblasts proliferate faster in the epidermis than in the dermis for all genotypes from E13.5, and the mathematical model proposes values for the doubling time. This indicates that the surrounding environment is important for the proliferation of the cells. We estimated the doubling times of Δbcat epidermal and dermal melanoblasts to be 49 hours and 74 hours, respectively, and of bcat* epidermal and dermal melanoblasts to be 23 hours and 31 hours, respectively (Table 1). Melanoblasts in the dermis interact mostly with fibroblasts and those in the epidermis, mostly with keratinocytes. Both interactions are mostly mediated by cadherins. The lack of β-catenin in melanoblasts affects E-cadherin localization at the cell-cell contact and influences Mitf-M expression (Fig. 7 and data not shown). The slight increase in β-catenin activity in bcat* melanoblasts does not affect cell-cell adhesion but increases signaling (Fig. 7 and data not shown). Consequently, the effects on the doubling time of bcat*

Table 1. Estimation of the doubling times (τ_θ) of dermal (de) and epidermal (ep) melanoblasts for each genotype based on an estimation of κ_θ at E14.5

	Δbcat		Wild type		bcat*	
	ep	de	ep	de	ep	de
τ mean	48.66	73.83	17.58	27.71	22.83	30.87
s.d.	1.04	24.20	0.23	8.59	0.41	6.39
τ min	35.71	49.55	17.29	18.03	22.68	23.24
τ max	49.55	148.66	18.03	54.09	23.23	43.90

The lower and upper bounds of κ_θ were deduced from BrdU experiments (see Fig. S4 in the supplementary material). These bounds allow the determination of the minimum (μ_θ min), maximum (μ_θ max) and average (μ_θ mean) rates of proliferation. From these rates of proliferation, τ_θ can be calculated using Eqn 3. The extreme values of the doubling times τ min and τ max calculated from the lower and upper bounds for κ_θ are indicated. On the basis of the mathematical model, we cannot formally exclude the possibility that κ_θ is equal to lower or upper bounds (these values are consistent with the model). However, biological data provides evidence that the proliferation rates of melanoblasts in the dermis are never higher than those in the epidermis. At E14.5, the rates of melanoblasts proliferation in the epidermis are higher than that in the dermis (see Fig. S4 in the supplementary material). Note that the minimum and maximum for the doubling times of Δbcat in the dermis are quite divergent. This is mainly due to the small numbers of melanoblasts in Δbcat mutant embryos.

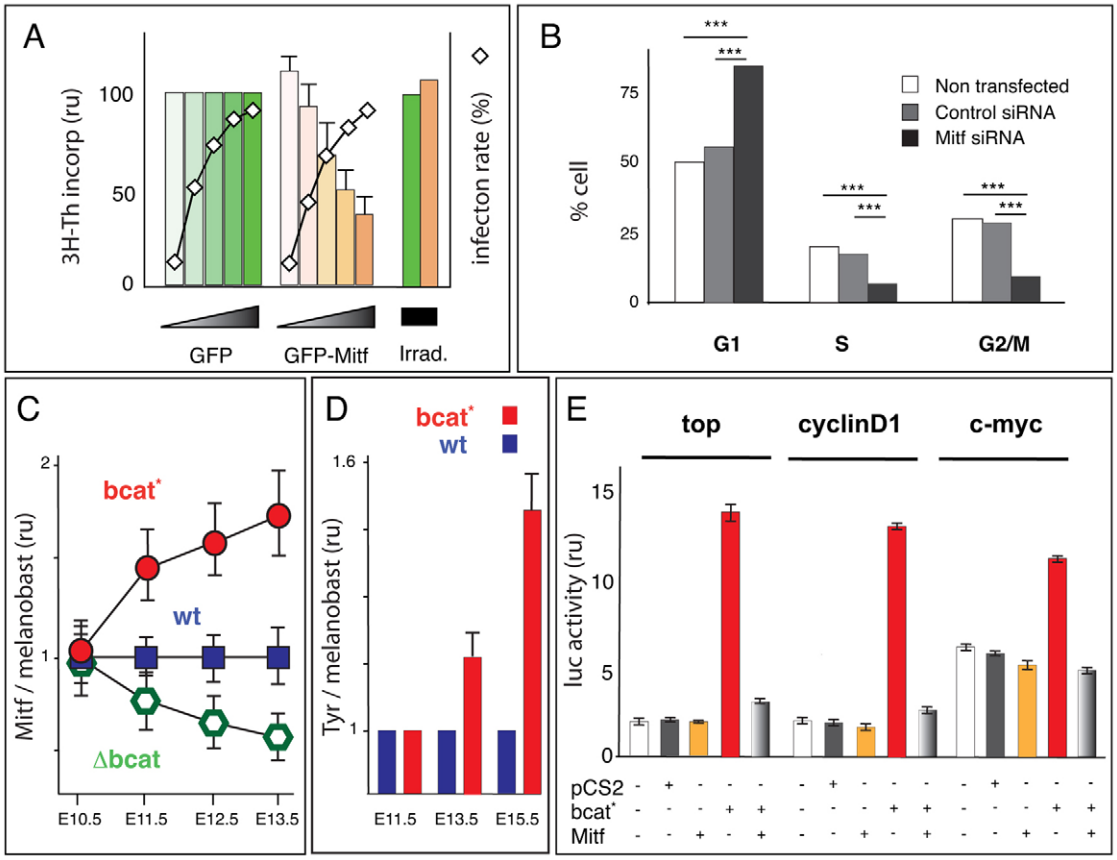

Fig. 7. A fine balance between β-catenin and Mitf levels is required for melanoblast proliferation. (**A**) FO-1 melanoma cells were infected with various amounts of adenoviruses encoding GFP-Mitf-M fusion protein and GFP as a control. The proliferation rate of FO-1 melanoma cells was arbitrary (ru), evaluated from thymidine incorporation. Percentages of infection were determined directly under a microscope equipped for epifluorescence (white diamonds, right panel). Adenovirus was inactivated for 1 hour at 56°C. (**B**) Melanoma cell lines were either transfected with control or Mitf siRNA or not transfected. The percentage of cells in each phase of the cycle (G1, S and G2/M) was evaluated by standard FACS analysis. ***$P<10^{-4}$. (**C**,**D**) The amount of Mitf-M (C) and tyrosinase (D) cDNA amplified from embryo skin is expressed relative to the number of melanoblasts. The Mitf-M (or Tyr) per melanoblast ratios for mutants are given relative to those for wild type defined as 1. Error bars indicate s.d. (**E**) Activities of top, cyclin D1 and Myc luciferase reporters in HEK293 cells, which do not produce Mitf, in the presence or absence of bcat* and/or Mitf-M. Three independent luciferase assays were performed in duplicate; errors bars represent s.d.

melanoblasts are likely to be mainly due to effects on β-catenin signaling, and the effects on the doubling time of Δbcat melanoblasts are presumably due to the lower β-catenin signaling and cell-cell adhesion.

Assuming that the doubling time of melanoblasts follows the same general rules during this period (E8.5 to E15.5), the number of founder melanoblasts (n^0; independent of κ_θ max (t)) can be estimated to be about 16 (for further details see the Appendix in the supplementary material). This means that on one side of the embryos there is roughly one founder melanoblast for about two somites. This value is consistent with the presence of a limited number of founder melanoblasts and with previous estimations (Mintz, 1967; Wilkie et al., 2002).

Mitf-M is regulated by the β-catenin level in melanoblasts

To investigate the molecular basis of the transcriptional effect of the β-catenin level on the proliferation of melanoblasts in vitro and in vivo, we analyzed the expression of *Mitf-M*, a specific target of β-catenin implicated in melanoblast and melanocyte proliferation. We analyzed the effect of an increasing amount of Mitf-M by infecting melanocytic cells in vitro with adenovirus expressing Mitf-M or, as a control, GFP. Cells infected with MITF-M showed less thymidine incorporation than controls (Fig. 7A), indicating that increasing the *Mitf-M* level inhibits cell proliferation. When the amount of Mitf-M was reduced in melanocytic cells in vitro by the use of an siRNA directed against Mitf (Fig. 7B), proliferation was affected and the length of G1 phase was clearly increased. These findings are consistent with previous in vitro studies (Carreira et al., 2005; Carreira et al., 2006). We then used Q-RT-PCR to determine the amount of *Mitf-M* mRNA per melanoblast in wild type and β-catenin mutant embryos (E10.5 to E13.5). At E10.5, wild-type and β-catenin-mutant melanoblasts contained similar amounts of *Mitf-M*. However, between E11.5 and E13.5, *Mitf-M* mRNA was more abundant in bcat* melanoblasts and less abundant in Δbcat melanoblasts than in wild-type melanoblasts (Fig. 7C). Thus, the level of *Mitf-M* gene expression correlates with the amount/activity of β-catenin in melanoblasts during development, indicating also that β-catenin is a major regulator of Mitf-M expression during melanoblast expansion. Furthermore, the upregulation of Mitf-M leads to an increase in tyrosinase expression in bcat* melanoblasts (Fig. 7D).

The increase in *Mitf-M* level may have an additional effect on melanoblast proliferation through its direct interaction with β-catenin. Indeed, the interaction between MITF-M and β-catenin can redirect β-catenin transcriptional activity toward Mitf-specific target genes (Schepsky et al., 2006). Although the effect of the MITF-M and β-catenin interaction was not investigated on natural β-catenin target genes, this finding suggests that transcriptional activation mediated by β-catenin in the melanocyte lineage may be modulated by the increased in MITF-M levels. To establish the effect of MITF-M on expression of the *Myc* and cyclin D1 genes, both well-known targets of β-catenin involved in proliferation, we evaluated their promoter activities in the presence of β-catenin with or without *Mitf-M* expression. We measured the activation of a luciferase reporter driven by the cyclin D1 and *Myc* promoters following expression of β-catenin, Mitf-M or both. The cyclin D1 and *Myc* promoter activities were stimulated by the presence of β-catenin, but Mitf-M expression alone had no effect. Interestingly, expression of Mitf-M abolished the transactivation driven by β-catenin (Fig. 7E). Therefore, the transactivation activity of β-catenin may be inhibited by an increased Mitf-M level. Possibly, cells expressing an activated form of β-catenin contain an increased level of Mitf-M, leading to a reduction in cyclin D1 and Myc, and consequently to a diminution in proliferation, which explains the phenotype observed in bcat* mice. In addition, in the absence of β-catenin, the transcription of all its targets is reduced leading to a severe proliferation defect in these cells, potentially explaining the phenotype observed in Δbcat mice.

DISCUSSION

Melanoblasts are a specific type of cell that displays extensive cellular proliferation during development. Melanoblasts colonize the dermis, epidermis and the hair follicle sequentially. In each compartment, they are exposed to a large variety of developmental cues. We show here that the number and the localization of melanoblasts are very well defined, resulting in tight control over melanoblast expansion, both spatially and temporally, with minimal variation in cell number and distribution in the skin. By paying careful attention to embryo stage and precise determination of melanoblast number, we revealed that melanoblast numbers were highly consistent from one embryo to another at any given stage. The model allowed estimation of the number of founder melanoblasts and the doubling time of melanoblasts in the dermis and the epidermis. To challenge the mathematical model, we used gain- and loss-of-function β-catenin mutants in a C57BL/6 background to modify β-catenin activity. β-Catenin is essential for the determination of the melanocyte lineage (Hari et al., 2002). Therefore, we modified β-catenin expression at around E10.5, after determination in this lineage. We showed that the gain-of-function using bcat* mice and the loss-of-function using Δbcat mice each led to a coat color phenotype: bcat* mice were hypopigmented and Δbcat mice were white. The lack of pigmentation for Δbcat mice was not so surprising in light of the functions of β-catenin in other lineages. However, the hypopigmentation observed in bcat* mice was puzzling. It appears that the modification of β-catenin production in both directions affects cell proliferation but does not interfere significantly with apoptosis or cell fate. In epithelial cells, cyclin D1 and Myc, two proteins promoting cell proliferation, can be directly induced by β-catenin. In melanocytes, in addition to *cyclin D1* and *Myc* another direct β-catenin target, *Mitf-M*, also controls cell proliferation (Bismuth et al., 2005; Carreira et al., 2005; Carreira et al., 2006; Garraway et al., 2005; Loercher et al., 2005). However, the only evidence that Mitf has a role in melanoblast proliferation in vivo is very indirect (Hornyak et al., 2001). We showed that the transcriptional activity of β-catenin on its cellular proliferative targets can be inhibited by Mitf-M. Thus, in bcat* melanoblasts, β-catenin induces the expression of Mitf-M, which in turn exerts a negative feed-back control by inhibiting β-catenin transcriptional activity on *cyclin D1* and *Myc* promoters, and therefore cell proliferation. By way of their close interconnection, β-catenin and MITF-M not only direct melanoblast cell fate but also coordinate cell proliferation during development.

Establishment of the melanocyte lineage

The localization and the number of melanoblasts during development were first studied by in situ hybridization using probes for Mitf, Kit, Pax3 and Sox10 (Thomas and Erickson, 2008). Subsequently, Dct::lacZ transgenic mice were used to visualize melanoblasts during development from E10.5 (Mackenzie et al., 1997). The use of Dct::lacZ mice appears to have a sensitivity similar to that of in situ hybridization experiments, but this method is faster and more convenient for double or triple staining. Previous studies indicated that melanoblast numbers increase substantially during development (Hornyak et al., 2001; Mackenzie et al., 1997; Silver et al., 2008; Van Raamsdonk et al., 2004). However, these various studies did not examine cell number or dermal/epidermal distribution in detail. After backcrossing Dct::lacZ mice towards C56BL/6 mice, we were able to provide a precise description of melanoblast number and location from E10.5 to E15.5. We focused our analysis on the trunk because this region shows less complexity in terms of melanoblast expansion than the cephalic, vagal or sacral regions; in particular, it has a lower density of melanoblast founders (Fig. 1) (Mackenzie et al., 1997; Wilkie et al., 2002).

After cell specification, melanoblasts spread and start to proliferate in the dermis. From E12.5 to E15.5, most of the cells in the dermis and epidermis are cycling (Ki67 positive, a marker of cycling cells, data not shown) and the number of melanoblasts in the dermis remains fairly constant. These cells are not dying or changing cell fate. These observations suggest that a regular flow of cells crosses the basement membrane between the dermis and epidermis. It suggests that the rate of migration from dermis to epidermis is similar to the rate of proliferation in the dermis. This is consistent with an asymmetric division of dermal melanoblasts: after each cell division, one cell stays in the dermis and one migrates to the epidermis. However, we cannot exclude the possibility that there is a constant rate of emigration without selectivity in which cell emigrate. How the flow of melanoblasts from the dermis to the epidermis is controlled remains unknown, but the following three parameters are undoubtedly involved: the intrinsic capacity of melanoblasts to pass from the dermis to the epidermis; attraction/repulsion of the melanoblasts that migrate from the dermis to the epidermis (including the chemo-attraction); and the quality of the basement membrane that separates the dermis from the epidermis. There is possibly asymmetric cell division such that one of the daughter cells is competent to cross the basement membrane immediately after mitosis (or at the beginning of G1) and the other daughter cell is not. The crossing daughter cells would then be those inheriting components that allow the migration from the dermis to the epidermis. These components may be linked (protein at the membrane) or not linked (a particular combination of transcription factors) to the shape of the cells and/or to local degradation of the basement membrane.

The first epidermal melanoblasts are observable at E11.5. This means that the flow from the dermis to the epidermis starts at around that time and continues until E15.5 or later. In the two β-catenin mutants used in this study, dermal melanoblasts in the embryos were cycling and the number of dermal melanoblasts remained constant. Therefore, β-catenin does not appear to affect the asymmetric division and does not seem to contribute to the control of melanoblast migration from the dermis to the epidermis.

Doubling time of dermal and epidermal melanoblasts

By E12.5, almost half of all melanoblasts are in the epidermal compartment where they proliferate actively. The increasing melanoblast count in the epidermis results from both the division of these cells in this compartment and the continuous flow of dermal melanoblasts. However, at later stages, the number of melanoblasts coming from the dermis is negligible compared with the number of melanoblasts proliferating in the epidermis. Using our experimental findings for melanoblast numbers and locations, we established a mathematical model of the proliferation of these cells in both skin compartments, allowing melanoblast doubling times to be estimated. Using this mathematical model, we were able to determine the in vivo doubling time of wild-type and mutant murine melanoblasts in two independent compartments (epidermis and dermis), which are separated by a physical barrier. We could determine the number of cells in each compartments at different time of development (from E11.5 to E15.5), but it is not yet technically possible to evaluate the flow of melanoblasts going from the dermis to epidermis. Other mathematical models have already been established to determine the proliferation features for cells in culture or in vivo (Chou et al., 2010; Di Garbo et al., 2010; Hyrien et al., 2010; Tabatabai et al., 2011; Tomasetti and Levy, 2010). However, none of them brings clear values of doubling times of their considered cells, as we do. They do not challenge their mathematical models with mutants, as we do. This challenge was certainly of a great importance. We first developed a linear model, which gave reproducible values for the doubling times of wild-type and bcat* melanoblasts. Unfortunately, this mathematical model was not reproducible and produced erratic results for Δbcat. We therefore decided to develop a generic mathematical model fitting any mouse mutant from white to black, with all possible intermediates. The mathematical model presented is nonlinear, which is biologically relevant. This nonlinear model generates reproducible values for the doubling times of wild-type, bcat* and Δbcat melanoblasts. It should be noted that the doubling time of wild-type melanoblasts was similar with both linear and non linear mathematical models. Similar findings were obtained for bcat* melanoblasts. The methodology developed here is a compromise between expected balance equations, behavior and feature extractions from data, and validation of data fitting. The mathematical model, combined with the biological information (BrdU experiments), indicated that melanoblasts proliferate more rapidly in the epidermis than in the dermis. In addition, using the β-catenin mutant mice, we could show that melanoblast proliferation would be dependent on cell-cell adhesion and signaling in both compartments. We conclude that both surrounding environment and genetic context influence the proliferation rate of melanoblasts during development. Those findings are consistent with those of Kunisada, suggesting that specific factors influence melanocyte survival/growth/differentiation as a function of their location in the skin (Aoki et al., 2009). This model provided no evidence, either mathematical or experimental, for a second major wave of melanoblast production, at the body location and stages of development analyzed (Adameyko et al., 2009; Jordan and Jackson, 2000).

A novel mathematical approach to evaluate the number of founder melanoblasts

The number of founder melanoblasts has been a subject of discussion over the years. This number has been estimated either by observing transversal coat color stripes in adult mice derived from aggregating morulae of various genetic backgrounds, or by analyzing melanoblast number/distribution revealed by X-gal staining in mosaic embryos (Mintz, 1967; Wilkie et al., 2002). We estimated that the doubling time of melanoblasts in the dermis between E10.5 and E15.5 was about 28 hours. If we assume that founder melanoblasts are determined at E8.5 in the truncal region and that the doubling times of progenitors and migrating melanoblasts are similar from E8.5 to E15.5, the mathematical model indicates that there are about 16 founder melanoblasts in the truncal region, which is consistent with previous genetic findings suggesting that there is a small number of founder melanoblasts in the trunk (Mintz, 1967). In the cephalic and vagal regions, we estimated that the number of founder melanoblasts would be larger, consistent with the findings of Wilkie et al. (Wilkie et al., 2002).

In conclusion, this biological and mathematical modeling may help to elucidate the function of mutated proteins during melanocyte development in a particular environment and can be used to predict the proliferative status of other genetically modified melanoblasts. In this specific case, the gain- and loss-of-function of β-catenin revealed that β-catenin affects melanoblast proliferation, but not migration from the dermis to the epidermis. Two other signaling pathways, those involving endothelin and Kitl and its receptor, are involved in the proliferation/survival of melanoblasts in the dermis and epidermis in vivo. It would be interesting to evaluate the respective importance of these three signaling pathways during the establishment of the melanocyte lineage.

Acknowledgements

We are grateful to I. Jackson for providing a mouse strain (*Dct::lacZ* mice) and to I. Davidson for comments on the manuscript. We thank all members of the animal colony and imaging facilities of Institut Curie. We also thank Y. Bourgeois, F. Cordelières and H. Harmange. We thank T. Eguether for technical assistance. F.L. was supported by fellowships from MENRT, SFD and LNCC-Essonnes. L.D. was supported by fellowships from LNCC-Oise and ARC. This work was supported by LNCC (Oise et Nationale – labellisation), INCa and Cancéropole IdF.

Competing interests statement

The authors declare no competing financial interests.

Supplementary material

Supplementary material for this article is available at
http://dev.biologists.org/lookup/suppl/doi:10.1242/dev.067447/-/DC1

References

Adameyko, I., Lallemend, F., Aquino, J. B., Pereira, J. A., Topilko, P., Muller, T., Fritz, N., Beljajeva, A., Mochii, M., Liste, I. et al. (2009). Schwann cell precursors from nerve innervation are a cellular origin of melanocytes in skin. *Cell* **139**, 366-379.

Aoki, H., Yamada, Y., Hara, A. and Kunisada, T. (2009). Two distinct types of mouse melanocyte: differential signaling requirement for the maintenance of non-cutaneous and dermal versus epidermal melanocytes. *Development* **136**, 2511-2521.

Aylaj, B., Luciani, F., Delmas, V., Larue, L. and De Vuyst, F. (2011). Melanoblast proliferation dynamics during mouse embryonic development. Modeling and validation. *J. Theor. Biol.* **276**, 86-98.

Bismuth, K., Maric, D. and Arnheiter, H. (2005). MITF and cell proliferation: the role of alternative splice forms. *Pigment Cell Res.* **18**, 349-359.
Brault, V., Moore, R., Kutsch, S., Ishibashi, M., Rowitch, D. H., McMahon, A. P., Sommer, L., Boussadia, O. and Kemler, R. (2001). Inactivation of the beta-catenin gene by Wnt1-Cre-mediated deletion results in dramatic brain malformation and failure of craniofacial development. *Development* **128**, 1253-1264.
Carreira, S., Goodall, J., Aksan, I., La Rocca, S. A., Galibert, M. D., Denat, L., Larue, L. and Goding, C. R. (2005). Mitf cooperates with Rb1 and activates p21Cip1 expression to regulate cell cycle progression. *Nature* **433**, 764-769.
Carreira, S., Goodall, J., Denat, L., Rodriguez, M., Nuciforo, P., Hoek, K. S., Testori, A., Larue, L. and Goding, C. R. (2006). Mitf regulation of Dia1 controls melanoma proliferation and invasiveness. *Genes Dev.* **20**, 3426-3439.
Chou, C. S., Lo, W. C., Gokoffski, K. K., Zhang, Y. T., Wan, F. Y., Lander, A. D., Calof, A. L. and Nie, Q. (2010). Spatial dynamics of multistage cell lineages in tissue stratification. *Biophys. J.* **99**, 3145-3154.
Delmas, V., Martinozzi, S., Bourgeois, Y., Holzenberger, M. and Larue, L. (2003). Cre-mediated recombination in the skin melanocyte lineage. *Genesis* **36**, 73-80.
Delmas, V., Beermann, F., Martinozzi, S., Carreira, S., Ackermann, J., Kumasaka, M., Denat, L., Goodall, J., Luciani, F., Viros, A. et al. (2007). Beta-catenin induces immortalization of melanocytes by suppressing p16INK4a expression and cooperates with N-Ras in melanoma development. *Genes Dev.* **21**, 2923-2935.
Di Garbo, A., Johnston, M. D., Chapman, S. J. and Maini, P. K. (2010). Variable renewal rate and growth properties of cell populations in colon crypts. *Phys. Rev. E Stat. Nonlin. Soft Matter Phys.* **81**, 061909.
Dorsky, R. I., Raible, D. W. and Moon, R. T. (2000). Direct regulation of nacre, a zebrafish MITF homolog required for pigment cell formation, by the Wnt pathway. *Genes Dev.* **14**, 158-162.
Du, J., Widlund, H. R., Horstmann, M. A., Ramaswamy, S., Ross, K., Huber, W. E., Nishimura, E. K., Golub, T. R. and Fisher, D. E. (2004). Critical role of CDK2 for melanoma growth linked to its melanocyte-specific transcriptional regulation by MITF. *Cancer Cell* **6**, 565-576.
Dunn, K. J., Williams, B. O., Li, Y. and Pavan, W. J. (2000). Neural crest-directed gene transfer demonstrates Wnt1 role in melanocyte expansion and differentiation during mouse development. *Proc. Natl. Acad. Sci. USA* **97**, 10050-10055.
Gaggioli, C., Busca, R., Abbe, P., Ortonne, J. P. and Ballotti, R. (2003). Microphthalmia-associated transcription factor (MITF) is required but is not sufficient to induce the expression of melanogenic genes. *Pigment Cell Res.* **16**, 374-382.
Garraway, L. A., Widlund, H. R., Rubin, M. A., Getz, G., Berger, A. J., Ramaswamy, S., Beroukhim, R., Milner, D. A., Granter, S. R., Du, J. et al. (2005). Integrative genomic analyses identify MITF as a lineage survival oncogene amplified in malignant melanoma. *Nature* **436**, 117-122.
Grigoryan, T., Wend, P., Klaus, A. and Birchmeier, W. (2008). Deciphering the function of canonical Wnt signals in development and disease: conditional loss- and gain-of-function mutations of beta-catenin in mice. *Genes Dev.* **22**, 2308-2341.
Hari, L., Brault, V., Kleber, M., Lee, H. Y., Ille, F., Leimeroth, R., Paratore, C., Suter, U., Kemler, R. and Sommer, L. (2002). Lineage-specific requirements of beta-catenin in neural crest development. *J. Cell Biol.* **159**, 867-880.
Hornyak, T. J., Hayes, D. J., Chiu, L. Y. and Ziff, E. B. (2001). Transcription factors in melanocyte development: distinct roles for Pax-3 and Mitf. *Mech. Dev.* **101**, 47-59.
Hyrien, O., Dietrich, J. and Noble, M. (2010). Mathematical and experimental approaches to identify and predict the effects of chemotherapy on neuroglial precursors. *Cancer Res.* **70**, 10051-10059.
Ikeya, M., Lee, S. M., Johnson, J. E., McMahon, A. P. and Takada, S. (1997). Wnt signalling required for expansion of neural crest and CNS progenitors. *Nature* **389**, 966-970.
Jordan, S. A. and Jackson, I. J. (2000). A late wave of melanoblast differentiation and rostrocaudal migration revealed in patch and rump-white embryos. *Mech. Dev.* **92**, 135-143.
Lamoreux, M. L., Delmas, V., Larue, L. and Bennett, D. C. (2010). *The Colors of Mice: A Model Genetic Network*. Hoboken, NJ: Wiley-Blackwell.
Larue, L., Dougherty, N., Bradl, M. and Mintz, B. (1993). Melanocyte culture lines from Tyr-SV40E transgenic mice: models for the molecular genetic evolution of malignant melanoma. *Oncogene* **8**, 523-531.
Le Douarin, N. M. and Kalcheim, C. (1999). *The Neural Crest*. Cambridge: Cambridge University Press.
Loercher, A. E., Tank, E. M., Delston, R. B. and Harbour, J. W. (2005). MITF links differentiation with cell cycle arrest in melanocytes by transcriptional activation of INK4A. *J. Cell Biol.* **168**, 35-40.
Mackenzie, M. A., Jordan, S. A., Budd, P. S. and Jackson, I. J. (1997). Activation of the receptor tyrosine kinase Kit is required for the proliferation of melanoblasts in the mouse embryo. *Dev. Biol.* **192**, 99-107.
Mayer, T. C. (1973). The migratory pathway of neural crest cells into the skin of mouse embryos. *Dev. Biol.* **34**, 39-46.
McGill, G. G., Haq, R., Nishimura, E. K. and Fisher, D. E. (2006). c-Met expression is regulated by Mitf in the melanocyte lineage. *J. Biol. Chem.* **281**, 10365-10373.
Mintz, B. (1967). Gene control of mammalian pigmentary differentiation. I. Clonal origin of melanocytes. *Proc. Natl. Acad. Sci. USA* **58**, 344-351.
Pla, P., Moore, R., Morali, O. G., Grille, S., Martinozzi, S., Delmas, V. and Larue, L. (2001). Cadherins in neural crest cell development and transformation. *J. Cell. Physiol.* **189**, 121-132.
Puig, I., Champeval, D., De Santa Barbara, P., Jaubert, F., Lyonnet, S. and Larue, L. (2009). Deletion of Pten in the mouse enteric nervous system induces ganglioneuromatosis and mimics intestinal pseudoobstruction. *J. Clin. Invest.* **119**, 3586-3596.
Schepsky, A., Bruser, K., Gunnarsson, G. J., Goodall, J., Hallsson, J. H., Goding, C. R., Steingrimsson, E. and Hecht, A. (2006). The microphthalmia-associated transcription factor Mitf interacts with beta-catenin to determine target gene expression. *Mol. Cell. Biol.* **26**, 8914-8927.
Silver, D. L., Hou, L., Somerville, R., Young, M. E., Apte, S. S. and Pavan, W. J. (2008). The secreted metalloprotease ADAMTS20 is required for melanoblast survival. *PLoS Genet.* **4**, e1000003.
Soriano, P. (1999). Generalized lacZ expression with the ROSA26 Cre reporter strain. *Nat. Genet.* **21**, 70-71.
Tabatabai, M. A., Bursac, Z., Eby, W. M. and Singh, K. P. (2011). Mathematical modeling of stem cell proliferation. *Med. Biol. Eng. Comput.* **49**, 253-262.
Takeda, K., Yasumoto, K., Takada, R., Takada, S., Watanabe, K., Udono, T., Saito, H., Takahashi, K. and Shibahara, S. (2000). Induction of melanocyte-specific microphthalmia-associated transcription factor by Wnt-3a. *J. Biol. Chem.* **275**, 14013-14016.
Thomas, A. J. and Erickson, C. A. (2008). The making of a melanocyte: the specification of melanoblasts from the neural crest. *Pigment Cell Melanoma Res.* **21**, 598-610.
Tomasetti, C. and Levy, D. (2010). Role of symmetric and asymmetric division of stem cells in developing drug resistance. *Proc. Natl. Acad. Sci. USA* **107**, 16766-16771.
Van Raamsdonk, C. D., Fitch, K. R., Fuchs, H., de Angelis, M. H. and Barsh, G. S. (2004). Effects of G-protein mutations on skin color. *Nat. Genet.* **36**, 961-968.
Wehrle-Haller, B. and Weston, J. A. (1995). Soluble and cell-bound forms of steel factor activity play distinct roles in melanocyte precursor dispersal and survival on the lateral neural crest migration pathway. *Development* **121**, 731-742.
Wilkie, A. L., Jordan, S. A. and Jackson, I. J. (2002). Neural crest progenitors of the melanocyte lineage: coat colour patterns revisited. *Development* **129**, 3349-3357.
Yajima, I., Belloir, E., Bourgeois, Y., Kumasaka, M., Delmas, V. and Larue, L. (2006). Spatiotemporal gene control by the Cre-ERT2 system in melanocytes. *Genesis* **44**, 34-43.
Yamaguchi, Y. and Hearing, V. J. (2009). Physiological factors that regulate skin pigmentation. *Biofactors* **35**, 193-199.
Yasumoto, K., Takeda, K., Saito, H., Watanabe, K., Takahashi, K. and Shibahara, S. (2002). Microphthalmia-associated transcription factor interacts with LEF-1, a mediator of Wnt signaling. *EMBO J.* **21**, 2703-2714.

Supplementary Appendix :

Mathematical model

It should be pointed out that we first developed a linear model, which gave reproducible values for the doubling times of wt and bcat* melanoblasts. Unfortunately, this mathematical model was not reproducible and gave erratic results for Δbcat. We therefore decided to develop a generic mathematical model fitting any mouse mutant from white to black, with all possible intermediates. The mathematical model presented is non linear, which is biologically relevant. This non linear model generates reproducible values for the doubling times of wt, bcat* and Δbcat melanoblasts. It should be noted that the doubling time of wt melanoblasts was similar with both linear and non linear mathematical models. Similar findings were obtained for bcat* melanoblasts. The methodology developed here is a compromise between expected balance equations, behavior and feature extractions from data, and validation of data fitting.

A) Basic equations expressing the biological assumption. The number of founder melanoblasts located in the MSA is $n_{d,\theta}(t)$, which is equal to n^0. At this time, there are no melanoblasts in the developing epidermis $n_{e,\theta}(0) = 0$. The number of melanoblasts in the dermis (d) and epidermis (e) at a particular time (t) of development are denoted $n_{d,\theta}(t)$ and $n_{e,\theta}(t)$, respectively. The parameter θ represents the dependence on β-catenin activity. The flow $\Phi(t)$ of melanoblasts from the dermis to the epidermis is, unfortunately, unknown and cannot currently be determined experimentally. The dynamics of dermal and epidermal melanoblasts are modeled by the differential system

$$\frac{dn_{d,\theta}}{dt} = \mu_{d,\theta}(t)n_{d,\theta}(t) - \Phi_\theta\left(t, n_{d,\theta}(t), n_{e,\theta}(t)\right) \quad [1]$$ and

$\frac{dn_{e,\theta}}{dt} = \mu_{e,\theta}(t) n_{e,\theta}(t) + \Phi_\theta\left(t, n_{d,\theta}(t), n_{e,\theta}(t)\right)$ [2] , where $\mu_{d,\theta}(t)$ and $\mu_{e,\theta}(t)$ are the proliferation rates in the dermis and epidermis, respectively. The doubling times $\tau_{e,\theta}(t)$ and $\tau_{e,\theta}(t)$ are linked to $\mu_{d,\theta}(t)$ and $\mu_{e,\theta}(t)$ according to formula $\tau_{d,\theta}(t) = \frac{\log(2)}{\mu_{d,\theta}(t)}$, $\tau_{e,\theta}(t) = \frac{\log(2)}{\mu_{e,\theta}(t)}$ [3].

B) Additional knowledge extracted from the data. We need to determine the unknown flow $\Phi(t)$ to close the system. From the data, it is possible to find relevant features to guide the modeling process: **1.** Let us denote the total number of melanoblasts $n_\theta(t) = n_{d,\theta}(t) + n_{e,\theta}(t)$. Data analysis showed that the quantity $\log\left(n_\theta(t)\right)$ is an almost linear increasing function of time.

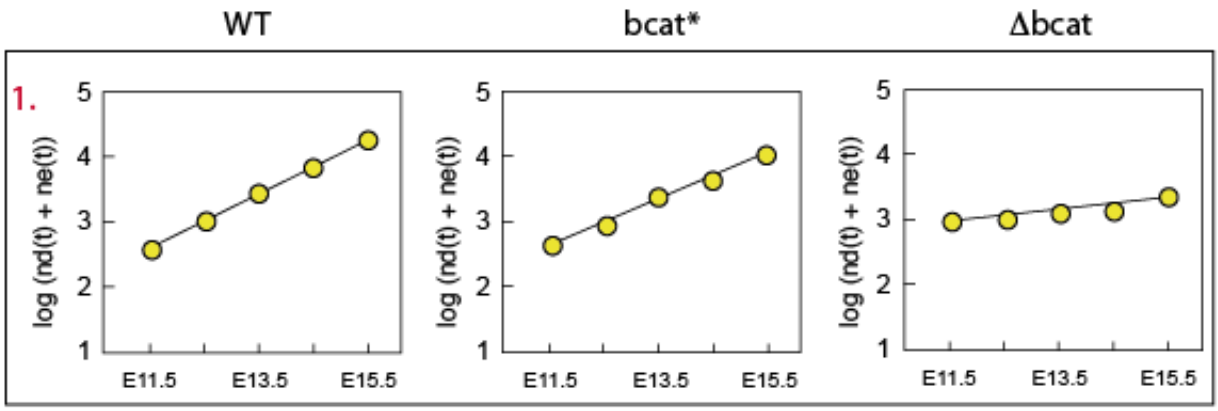

2. The fraction of melanoblasts in the dermis $y_\theta(t) = n_{d,\theta}(t)/n_\theta(t)$ was observed to behave as a decreasing sigmoid-shaped function of time. This allows us to postulate that $y_\theta(t)$ is the solution of a logistic-like differential equation $\frac{dy_\theta}{dt} = -\hat{c}_\theta(t) y_\theta(t)\left(1 - y_\theta(t)\right)$ [13].

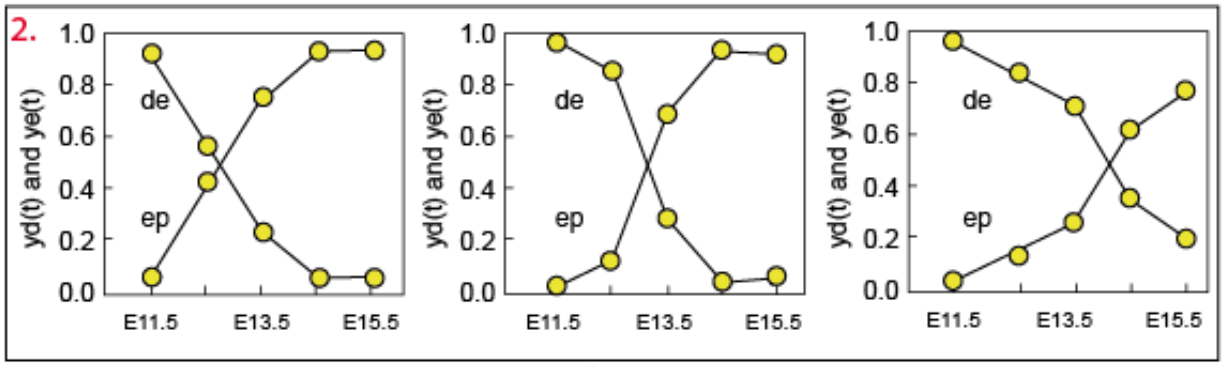

3. It was also observed that the quantity $\log\left(n_{e,\theta}(t)/n_{d,\theta}(t)\right)$, obtained from biological data, was a quasi-linear increasing function of time.

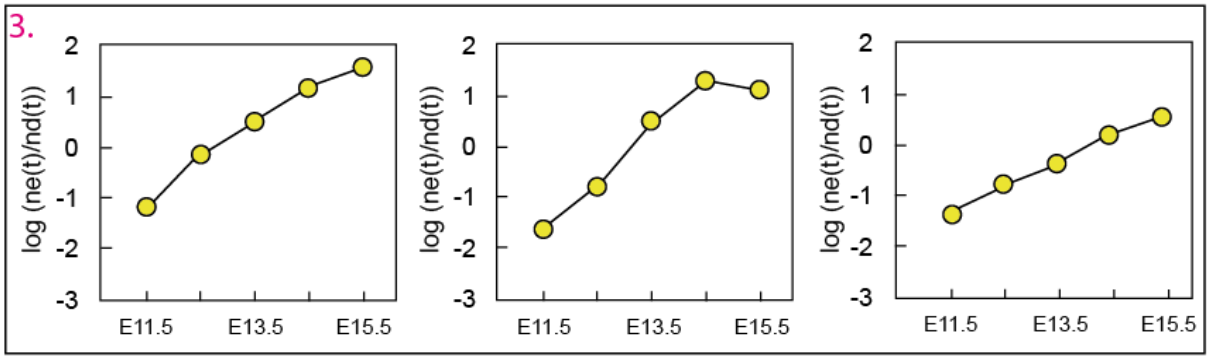

C) Modeling of the flow term. From these observations and extracted features, the system [1] and [2] can be rewritten using the variables of interest $n_\theta(t)$ and $y_\theta(t)$. We get $\frac{dn_\theta(t)}{dt} = \mu_\theta(t)n_\theta(t)$ [14] and $\frac{dy_\theta(t)}{dt} = -\left(\mu_{d,\theta} - \mu_{e,\theta}\right)y_\theta(t)\left(1-y_\theta(t)\right) - \frac{\Phi_\theta(t)}{n_\theta(t)}$ [15] where $\mu_\theta(t) = \left(y_\theta(t)\right)\mu_{d,\theta}(t) + \left(1-y_\theta(t)\right)\mu_{e,\theta}(t)$. This can also be expressed as $\frac{d\log\left(n_{e,\theta}(t)/n_{d,\theta}(t)\right)}{dt} = \mu_{e,\theta}(t) - \mu_{d,\theta}(t) + \frac{\Phi_\theta(t)}{y_\theta(t)\left(1-y_\theta(t)\right)n_\theta(t)}$ [16]. As $\mu_{d,\theta}(t)$ and $\mu_{e,\theta}(t)$ are expected to be bounded and $d\log\left(n_{e,\theta}(t)/n_{d,\theta}(t)\right)/dt$ is observed to vary slowly, the last term in equation [16] must also be bounded. Thus, we decided to close the flux term $\Phi(t)$ as $\Phi_\theta(t) = \kappa_\theta(t)y_\theta(t)\left(1-y_\theta(t)\right)n_\theta(t)$ [17] where $\kappa_\theta(t)$ is a smooth bounded function, which is still unknown but expected to vary slowly in time. In this case, combining equation [15] with

the closure [17] gives [13] with $c_\theta(t) = \mu_{e,\theta}(t) - \mu_{d,\theta}(t) + \kappa_\theta(t)$. Equation $\frac{dy_\theta}{dt} = -c_\theta(t) y_\theta(t)\left(1 - y_\theta(t)\right)$ [13] is a logistic equation and thus is able to produce sigmoid-like solutions as observed in the data.

D) Estimation of *c* and *mu*. Finally, combining [17] with equation [16] gives $c_\theta(t) = d\log\left(n_{e,\theta}(t)/n_{d,\theta}(t)\right)\Big/dt$ [7]. Equation [1] can be exploited to estimate the function $c_\theta(t)$ from the data. We will denote its estimator $\hat{c}_\theta(t)$. Similarly, equation [14] can be rewritten $d\log\left(n_\theta(t)\right)\Big/dt = \mu_\theta(t)$ [6]. Numerical experiments show that both $\mu(t)$ and $c(t)$ are smooth functions of time. Correct fitting to the data fitting requires an accurate estimation of these functions. Typically, the ratio between the maximum and the minimum of these functions is 10.

E) Final system used to estimate the number of founder melanoblasts. Note that the system can be completely closed without any dependence on the unknown function $\kappa_\theta(t)$:

$$\frac{dn_{d,\theta}(t)}{dt} = \hat{\mu}_\theta(t) n_{d,\theta}(t) - \hat{c}_\theta(t)\frac{n_{d,\theta}(t) n_{e,\theta}(t)}{n_{d,\theta}(t) + n_{e,\theta}(t)} \quad [18]$$

and

$$\frac{dn_{e,\theta}(t)}{dt} = \hat{\mu}_\theta(t) n_{e,\theta}(t) - \hat{c}_\theta(t)\frac{n_{d,\theta}(t) n_{e,\theta}(t)}{n_{d,\theta}(t) + n_{e,\theta}(t)} \quad [19]$$

. Once the functions $c_\theta(t)$ and $\mu_\theta(t)$ are estimated, it appears that the system [18] & [19] is able to give solutions that fit the data almost perfectly using standard estimation algorithms. To evaluate the number of founder melanoblasts, we initially interpolated the slope as is to earlier time from the WT curve. The values obtained were between 15 and 25. To avoid any stringency, we applied an inferior bound of 10 and superior bound of 50. In the second round, the number of founder melanoblasts was estimated by solving an inverse problem using least square minimization

given by $\min_{n_0,\, 10 \le n_0 \le 50} \sum_{i=E10.5}^{E15.5} \frac{1}{2\sigma_i^2}\left(n^{meas,i} - n^i(n_0)\right)^2$. The standard deviations σ_i are weighting variables that takes into account the errors associated with the data. For each mouse type, we computed an initial fraction y. We found $y^0 = 1 - 810^{-4}$. Obviously, " 8 10^{-4} " has no biological reality because at E8.5, at early developmental stage, stochastic and discrete dynamics are predominant. This value is, however, important to allow correct fitting. Regarding the number of founders, the estimation process returns a value of 16 ± 0.1 for each mouse type. This means that on one side of the embryos there is roughly one founder melanoblast for about two somites. The uncertainty about the value is related to the model uncertainty, which unfortunately cannot be quantified. The uncertainty is undoubtedly relatively large because a continuous differential model is used to represent the stochastic discrete dynamics in this early development stage.

F) Compatibility relationship of proliferation rate and the unknown kappa function. Equations [7] and [6] can be used to estimate both the function $c_\theta(t)$ and $\mu_\theta(t)$ from the data. We denote their estimators $\hat{c}_\theta(t)$ and $\hat{\mu}_\theta(t)$. Once the estimators $\hat{c}_\theta(t)$ and $\hat{\mu}_\theta(t)$ are computed using [7] & [6], we obtain the algebraic compatibility equations $\hat{c}_\theta(t) = \kappa_\theta(t) + \mu_{e,\theta}(t) - \mu_{d,\theta}(t)$ [4] and $\hat{\mu}_\theta(t) = \left(y_\theta(t)\right)\mu_{d,\theta}(t) + \left(1 - y_\theta(t)\right)\mu_{e,\theta}(t)$ [5]. Another result is that the determination of doubling times in the dermis and epidermis is an ill-posed problem from a deterministic point of view. At a given time, the system of algebraic equations [4] and [5] is underdetermined, with two equations and three unknowns $\mu_{d,\theta}(t)$, $\mu_{e,\theta}(t)$ and $\kappa_\theta(t)$. If $\kappa_\theta(t)$ can be estimated, then $\mu_{d,\theta}(t)$ and $\mu_{e,\theta}(t)$ can be determined. Rearranging the terms into [4] and [5] gives $\mu_{d,\theta}(t) = \hat{\mu}_\theta(t) - \left(1 - y_\theta(t)\right)\left(\hat{c}_\theta(t) - \kappa_\theta(t)\right)$ [9] and $\mu_{e,\theta}(t) = \hat{\mu}_\theta(t) + y_\theta(t)\left(\hat{c}_\theta(t) - \kappa_\theta(t)\right)$ [8].

G) Estimation of the doubling time according to relevant biological constraints. A rough estimation of $\kappa_\theta(t)$ can be obtained by adding a priori knowledge about doubling times. A priori biological knowledge about doubling times, in particular $\tau_{e,\theta}(t) \le \tau_{d,\theta}(t)$ and, $\tau_{d,\theta}(t) \le 3\tau_{e,\theta}(t)$ allows us to set bounds for the random variable $\kappa_\theta(t)$. Under the assumption $\tau_{e,\theta}(t) \le \tau_{d,\theta}(t)$, we have $\mu_{d,\theta}(t) \le \hat{\mu}_\theta(t) \le \mu_{e,\theta}(t)$ and then from [9] & [8] we get the inequality $\kappa_\theta(t) \le \hat{c}(t)$. A second a priori constraint gives the lower bound on $\kappa_\theta(t)$; $\kappa_\theta(t) \ge \left(\hat{c}_\theta(t) - 2\mu_\theta(t)/3 - 3y_\theta(t)\right)$.

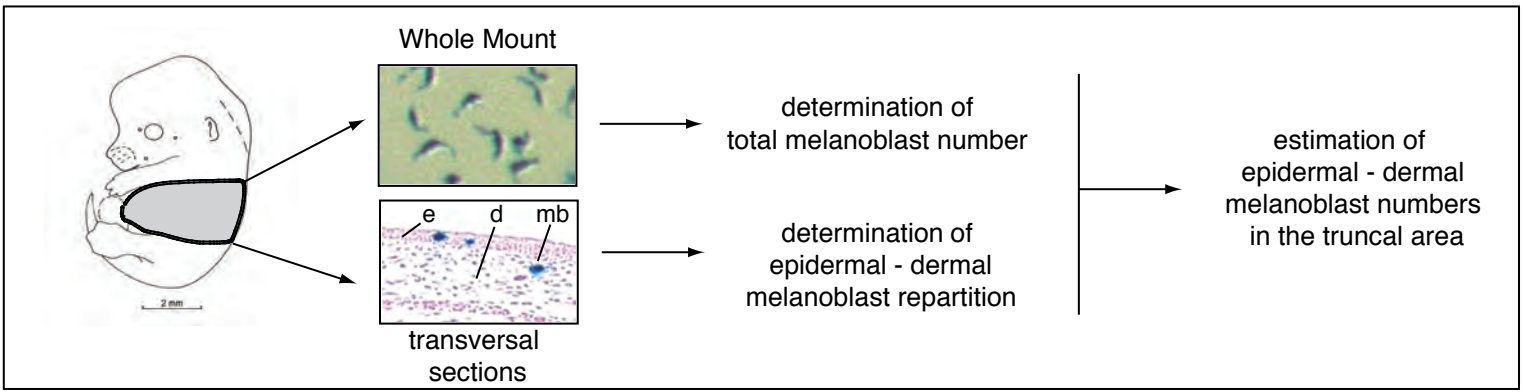

Figure S1: Determination of the number of melanoblasts
Melanoblasts were identified as X-gal-positive cells and were counted in the truncal region between the front and back limbs, from somites 13-25. The number of melanoblasts (mb) was determined from whole mount (wm) and sectioned (s) embryos previously stained with Xgal. epidermis (e), dermis (d).

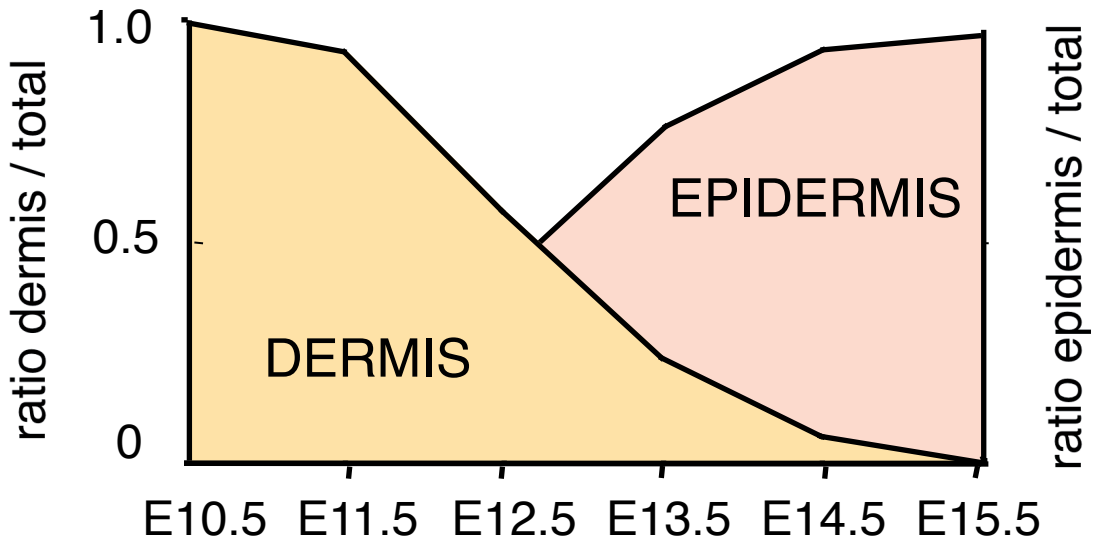

Figure S2: Distribution of epidermal and dermal melanoblasts in the two compartments during development.
In the truncal region, melanoblasts start to penetrate into the epidermis on E11.5, and most are located in this compartment by E15.5.

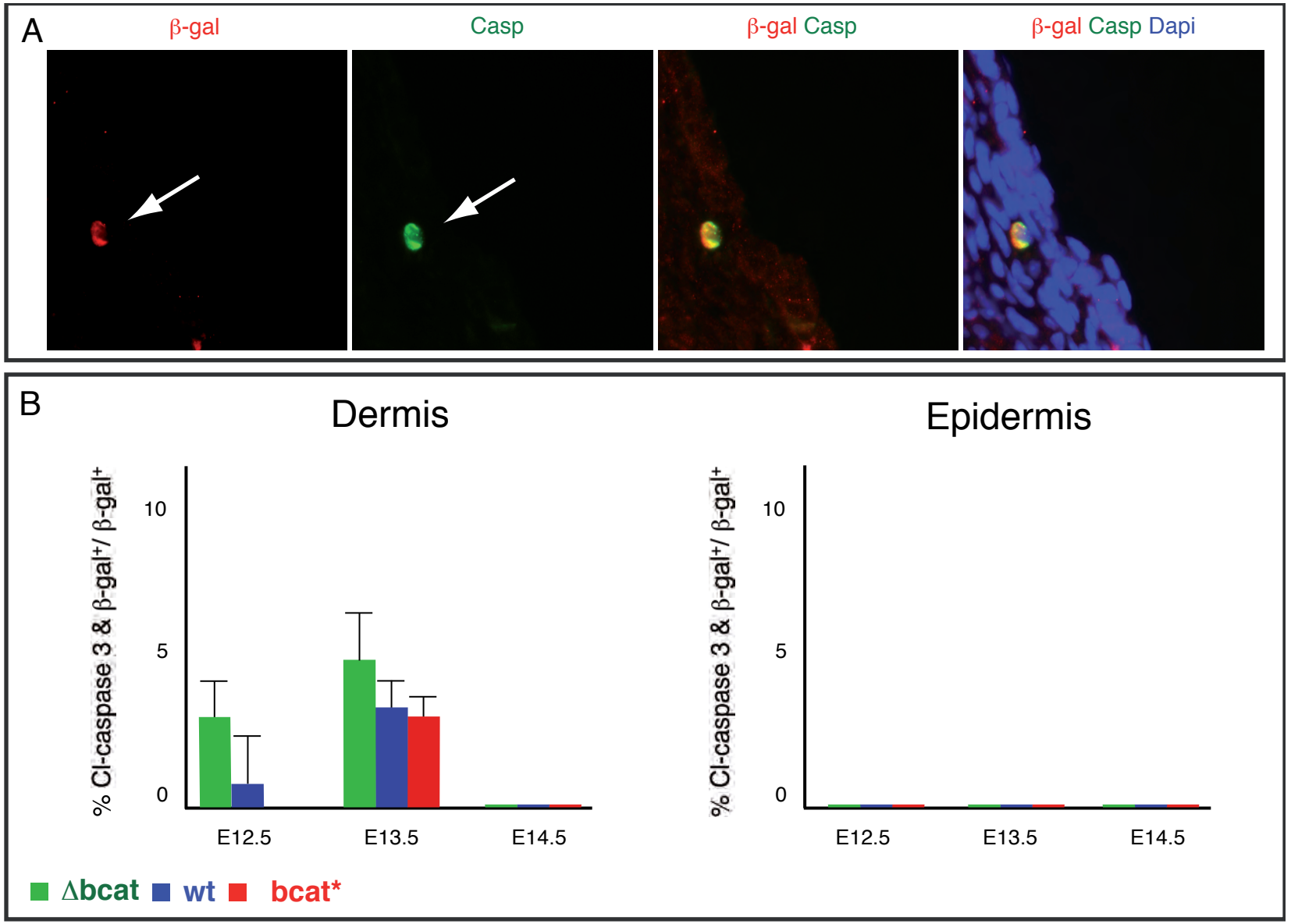
A
β-gal
Casp
β-gal Casp
β-gal Casp Dapi
B
Dermis
Epidermis
% Cl-caspase 3 & β-gal+/ β-gal+
10
5
0
E12.5
E13.5
E14.5
Δbcat
wt
bcat*

Figure S3: Detection of apoptotic melanoblasts in β-catenin mutants

Immunostaining of frozen E13.5 embryo sections, using anti-β-galactosidase (staining melanoblasts in red) and anti-cleaved caspase 3 antibodies (staining apoptotic cells in green). Images are merged to reveal apoptotic melanoblasts. (B) Quantification of apoptotic epidermal and dermal melanoblasts between E12.5 and E14.5 in Δbcat, wt, and bcat* embryos. Note that no apoptotic melanoblasts were detected in mice of any of the three genotypes.

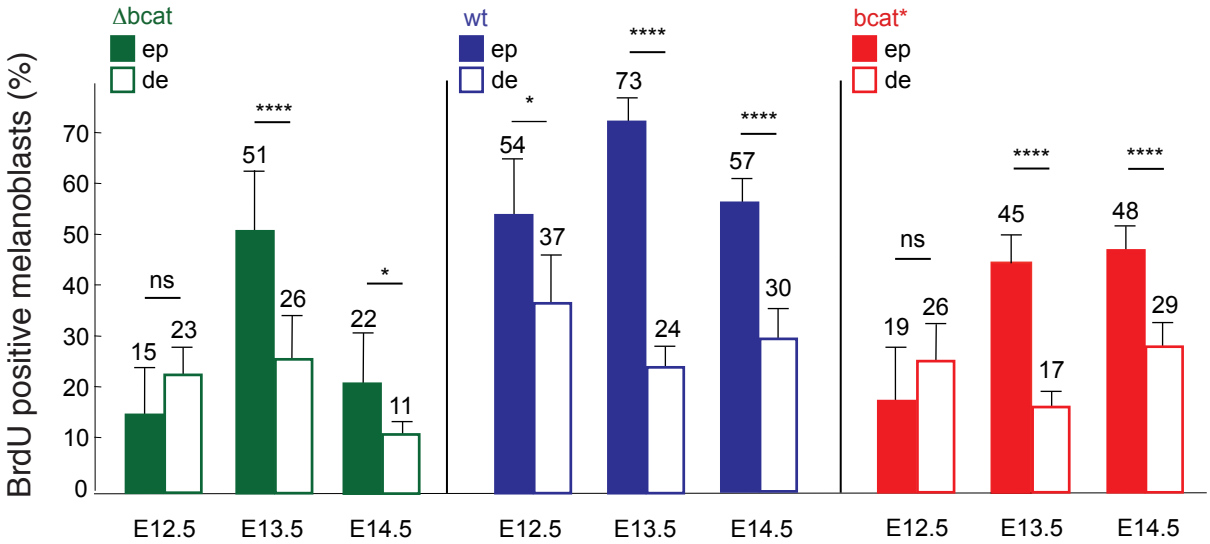
Δbcat
ep
de
wt
ep
de
bcat*
ep
de
BrdU positive melanoblasts (%)
0
10
20
30
40
50
60
70
ns
23
15
****
51
26
*
22
11
*
54
37
****
73
24
****
57
30
ns
19
26
****
45
17
****
48
29
E12.5
E13.5
E14.5
E12.5
E13.5
E14.5
E12.5
E13.5
E14.5

Figure S4. Establishing bounds to evaluate $\kappa_\theta(t)$

The proliferation rate of melanoblasts between E12.5 and E14.5 in Δbcat, wt and bcat* embryos was evaluated from BrdU incorporation experiments (see Figure 5). Statistical significance was calculated by comparing the proliferation rate of epidermal and dermal melanoblasts for each genotype at each stage with the Mann-Whitney test (StatEL) and is indicated, **** : p-value < 10^{-5}, * : p-value < 10^{-2}, ns=non significant. The proliferation rate of melanoblasts in the epidermis and that in the dermis were not significantly different at E12.5 for Δbcat and bcat* ($\tau_e = \tau_d$). With this exception, the proliferation rates of melanoblasts differed significantly between the dermis and epidermis on all developmental days and for each genotype (at least p < 10^{-2}). The proliferation rate is inversely correlated to the doubling time, so the doubling times of melanoblasts in epidermis are shorter than or similar to those in the dermis ($\tau_e \leq \tau_d$). An upper limit was established from biological findings. At this stage, cells are expected to be uniformly distributed around the cell cycle. BrdU labels cells in the S phase, such that the proportion of BrdU-positive cells indicates the proportion of cells in S phase. Assuming that the S phase is of similar length in the dermis and epidermis, then the relative lengths of the cell cycles can be estimated (%BrdU-positive in epidermis / %BrdU-positive in dermis). Experimentally, we found that %BrdU-positive in epidermis / %BrdU-positive in dermis was never greater than 3, such that $3\mu_d \geq \mu_e$. Indeed, in every case, τ_d was found to be lower than $3\tau_e$ (Δbcat : 74 h < 147 h [3*49], for wt 28h < 54 h [3*18] and for bcat* 31h < 69 h [3*23]).

These limits allow for bounds to be established for the unknown function $\kappa_\theta(t)$ by comparing the proliferation rate of melanoblasts between E12.5 and E14.5 in Δbcat, wt and bcat* embryos. Because of the uncertainty on the κ function, each $\kappa(t^i)$ at development day $E(t^i)$ was modeled as a random variable. As a first assessment, we decided to use Gaussian variables only involving expectation (E) values of $\kappa(t^i)$ and standard deviations of $\kappa(t^i)$. Both expectation values and standard deviations were roughly estimated from the bounds on

the κ function $E\left(\kappa\left(t_i\right)\right)=\frac{\kappa_{\min}\left(t_i\right)+\kappa_{\max}\left(t_i\right)}{2}$ and $\sigma_i=\frac{\kappa_{\max}\left(t_i\right)-\kappa_{\min}\left(t_i\right)}{2}$. The values obtained were reproducible and were biologically sound. This allowed us to design $\kappa(t)$ as random variable, Kmin ≤ K ≤ Kmax, which is $\max\left(0,\hat{c}(t)-\frac{2}{3-3y_\theta(t)}\hat{\mu}(t)\right)\le\kappa_\theta(t)\le\hat{c}(t)$. Bars represent standard deviation. Therefore $\kappa_\theta\min(t)=\max\left(0,\,c_\theta(t)-2\mu_\theta(t)/3-3y_\theta(t)\right)$ and $\kappa_\theta\max(t)=c_\theta(t)$. These two equations are derived from the following steps : starting from $3\mu_{d,\theta}\ge\mu_\theta$, then $\mu_{d,\theta}-\mu_\theta\ge-2\mu_\theta/3$, then $\left(\mu_{d,\theta}-\mu_\theta\right)/\left(1-y_\theta\right)\ge-2\mu_\theta/\left(3-3y_\theta\right)$, and $\mu_{d,\theta}-\mu_\theta=-\left(1-y_\theta\right)\left(c_\theta-\kappa_\theta\right)$ [9], then $\kappa_\theta\ge c_\theta-2\mu_\theta/\left(3-3y_\theta\right)$, therefore $\kappa_\theta\min=c_\theta-2\mu_\theta/\left(3-3y_\theta\right)$. Starting from $\mu_{d,\theta}=\mu_\theta-\left(1-y_\theta\right)\left(c_\theta-\kappa_\theta\right)$ [9] and $\mu_{\theta,d}\le\mu_\theta$, then $\kappa_\theta=c_\theta+\left(\mu_{d,\theta}-\mu_\theta\right)/\left(1-y_\theta\right)$, and then $\kappa_\theta\max(t)=c_\theta(t)$.

	embryonic stage	nb of embryos which were sectioned	nb of sections	average nb of total (ep+de) mb/section ($n_{t/s}$)	average nb of mb defined by whole mount (n_{wm})	average nb of ep mb/section ($n_{e/s}$)	ratio of ep mb/total mb (%) ($n_{e/s}/n_{t/s}$)	estimated nb of ep mb ($n_e = n_{wm} \times n_{e/s} / n_{t/s}$)	average nb of de mb/section ($n_{d/s}$)	ratio of de mb/total mb (%) ($y = n_{d/s}/n_{t/s}$)	estimated nb of de mb ($n_d = n_{wm} \times n_{d/s} / n_{t/s}$)
WT	E10.5	-	-	-	98	-	0.00	0	-	100.00	98
	E11.5	4	138	7.54	393	0.50	6.63	26	7.04	93.37	367
	E12.5	4	118	23.40	1,062	10.00	42.74	454	13.40	57.26	608
	E13.5	4	116	44.86	2,874	34.17	76.17	2,189	10.69	23.83	685
	E14.5	4	137	129.63	7,259	121.83	93.98	6,822	7.80	6.02	437
	E15.5	2	66	329.70	18,543	320.32	97.15	18,014	9.38	2.85	529
Δbcat	E10.5	-	-	-	106	-	-	0	-	100.00	106
	E11.5	2	54	9.82	533	0.20	0.02	11	9.62	97.96	522
	E12.5	2	55	11.34	715	1.65	14.55	104	9.69	85.55	611
	E13.5	2	54	11.35	791	3.10	27.31	216	8.25	72.69	575
	E14.5	2	65	8.62	1,000	5.45	63.23	632	3.17	36.77	368
	E15.5	2	69	10.44	1,510	8.22	78.74	1,188	2.21	21.26	321
bcat*	E10.5	-	-	-	95	-	0.00	0	-	100.00	95
	E11.5	4	118	2.43	278	0.05	2.06	6	2.38	97.94	272
	E12.5	2	56	5.95	773	0.79	13.28	103	5.16	86.72	670
	E13.5	2	56	10.03	1,452	7.57	75.47	1,096	2.46	24.53	356
	E14.5	2	41	20.24	2,578	19.24	95.06	2,451	1.00	4.94	127
	E15.5	2	53	79.58	6,302	73.98	92.96	5,858	5.60	7.04	443

mb=melanoblast; nb=number; e=epidermis; d=dermis

Table S1: Determination of the number of melanoblasts

The number (nb) of melanoblasts (mb) was determined from whole mount (wm) and sectioned (s) embryos previously stained with Xgal. Between 41 and 138 sections from 2-4 embryos were analyzed at each stage of development. n_{wm} is the mean number of melanoblasts assessed from whole mounts (wm). $n_{e/s}$, $n_{d/s}$ and $n_{t/s}$ are the mean numbers of epidermal (e), dermal (d) and total $(t = e + d)$ melanoblasts per section (s), respectively. n_e and n_d are the numbers of melanoblasts in epidermis and dermis, respectively, on a given embryonic day. They were calculated as follows: $n_e = n_{WM} \, x \, n_{e/s} / n_{t/s}$ and $n_d = n_{WM} \, x \, n_{d/s} / n_{t/s}$.

For data from whole mounts, note that the mean values are almost identical to the median values: mean and median on embryonic day 10.5 (E10.5) are 98 and 100, respectively, on E11.5 (393 and 364), on E12.5 (1,062 and 900), on E13.5 (2,874 and 2,908), on E14.5 (7,259 and 7,080) and on E15.5 (18,543 and 19,907).

For data from sections, note that the mean and median are for Δbcat on E10.5 (106 and 104), on E11.5 (533 and 556), on E12.5 (715 and 718), on E13.5 (791 and 705), on E14.5 (1,000 and 1,100) and on E15 (1,510 and 1,400), and for bcat* on E10.5 (95 and 95), on E11.5 (278 and 254), on E12.5 (773 and 773), on E13.5 (1,452 and 1,530), on E14.5 (2,578 and 2,551) and on E15.5 (6,302 and 6,497).